FT-2: Magneto-optics and Magneto-plasmonics Part 1

P. Vavassori

-Ikerbasque, Basque Fundation for Science and CIC nanoGUNE Consolider, San Sebastian, Spain.

THE EUROPEAN SCHOOL ON
MAGNETISM 2018
MAGNETISM BY LIGHT

Outline

Magneto-optics

Brief overview of the Magneto-optical Kerr effects (MOKE)
Advanced MOKE: vector magnetometry

Magnetic nanostructures

micro-MOKE

Approach 1: focused beam
Approach 2: microscopy

MOKE from diffracted beams:

simple theory of diffracted MOKE
in conjunction with micromagnetics and MFM
from magnetometry to magnetic imaging

The MagnetoOptical Effect

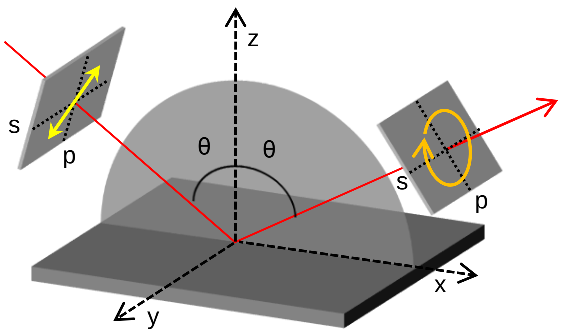

$$R = \begin{pmatrix} r_{s\to s} & \\ & r_{p\to p} \end{pmatrix}$$

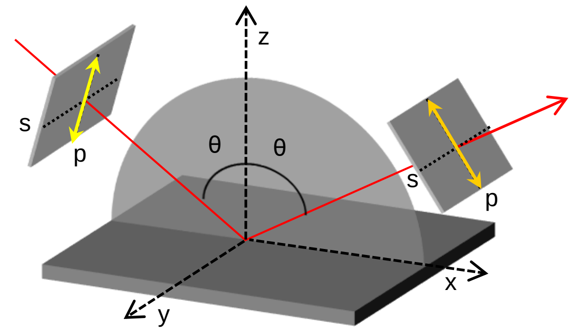

But, what happens if we applied a **magnetic field??**

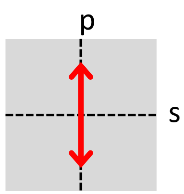

Polarization Plane

Sample

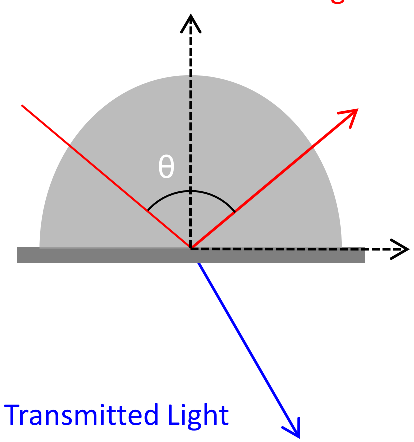

Reflected Light

Transmitted Light

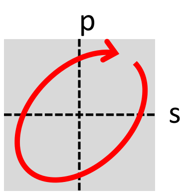

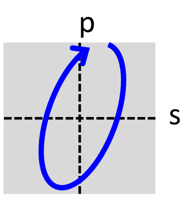

John Kerr
1824 - 1907

Michael Faraday
1791 - 1867

The Magneto-Optical Effect

Polar and Longitudinal Configuration

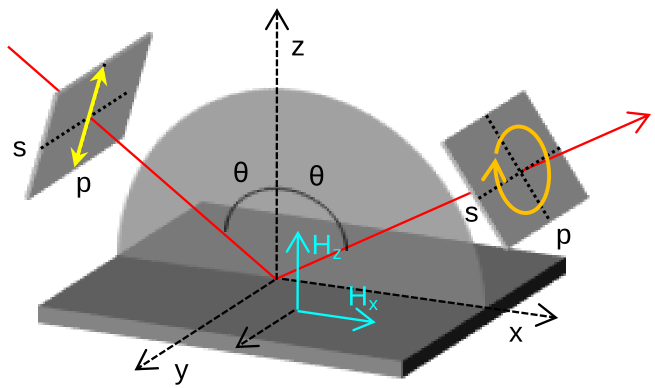

Transverse Configuration

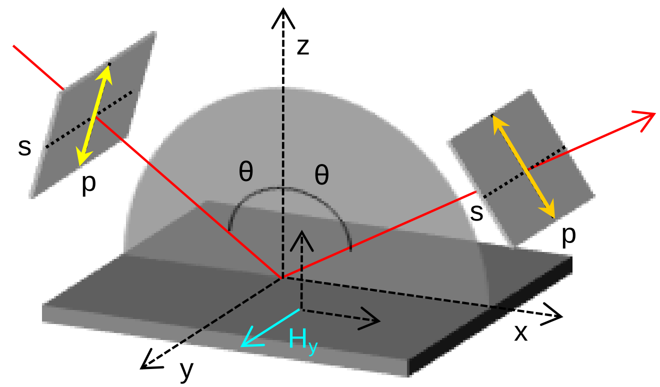

Dielectric Tensor

$$\begin{pmatrix} \varepsilon_{xx} & \varepsilon_{xy} & \varepsilon_{xz} \\ \varepsilon_{yx} & \varepsilon_{yy} & \varepsilon_{yz} \\ \varepsilon_{zx} & \varepsilon_{zy} & \varepsilon_{zz} \end{pmatrix}$$

Reflectivity matrix

$$R = \begin{pmatrix} r_{s\to s} & r_{p\to s} \\ r_{s\to p} & r_{p\to p} \end{pmatrix}$$

MOKE

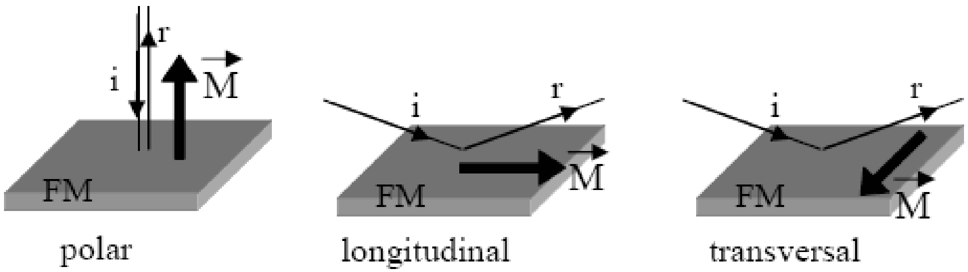

The magneto-optic Kerr effect (MOKE) is widely used in studying technologically relevant magnetic materials.

It relies on small, magnetization induced changes in the optical properties which modify the polarization or the intensity of the reflected light.

Macroscopically, magneto-optic effects arise from the antisymmetric, off-diagonal elements in the dielectric tensor.

$$\hat{\varepsilon} = \begin{bmatrix} \varepsilon_0 & 0 & 0 \\ 0 & \varepsilon_0 & 0 \\ 0 & 0 & \varepsilon_0 \end{bmatrix} \Rightarrow \hat{\varepsilon} = \begin{bmatrix} \varepsilon_0 & i\varepsilon_z & -i\varepsilon_y \\ -i\varepsilon_z & \varepsilon_0 & i\varepsilon_x \\ i\varepsilon_y & -i\varepsilon_x & \varepsilon_0 \end{bmatrix}$$

$$\varepsilon_x = \varepsilon_0 Q\, m_x;\ \varepsilon_y = \varepsilon_0 Q\, m_y;\ \varepsilon_z = \varepsilon_0 Q\, m_z;$$

- **Non-destructive;**
- **High sensitivity;**
- **Finite penetration depth (~ 10 nm);**
- **Fast (time resolved measurements);**
- **Laterally resolved (microscopy);**
- **Can be easily used in vacuum and cryogenic systems;**

J. Kerr, Philosophical Magazine **3** 321 (1877)
Z. Q. Qui and S. D. Bader, Rev. Sci. Instrum. **71,** 1243 (2000)

Fresnell reflection coefficients

Sample $\begin{pmatrix} r_{pp} & r_{ps} \\ r_{sp} & r_{ss} \end{pmatrix}$

$r_{pp} = r^0_{pp} + r_{pp}^M \propto m_y$
$r_{ps} \propto - m_x - m_z$
$r_{sp} \propto m_x - m_z$

$$r_{pp} = \frac{E_{rTM}}{E_{iTM}} \qquad r_{ps} = \frac{E_{rTM}}{E_{iTE}} \qquad r_{sp} = \frac{E_{rTE}}{E_{iTM}} \qquad r_{ss} = \frac{E_{rTE}}{E_{iTE}}$$

P. Vavassori, APL 77 1605 (2000)

MOKE origin: classical picture Lorentz force

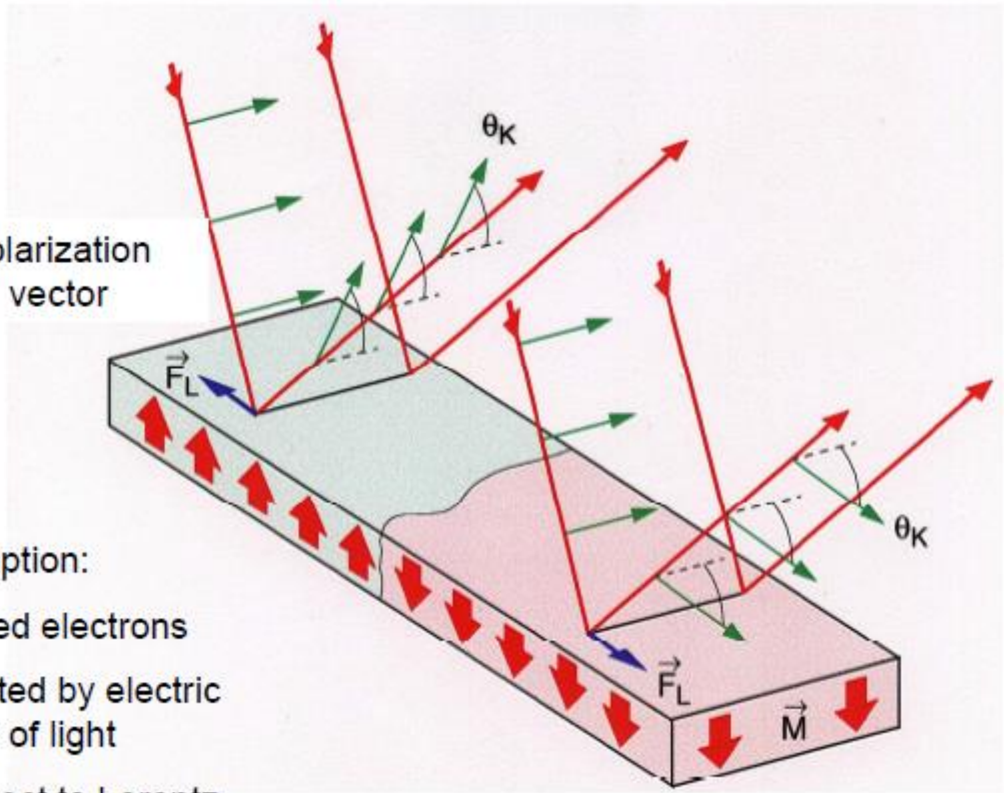

Assumption:

localized electrons

- excited by electric field of light
- subject to Lorentz force

Electron theory of Magneto-Optics

Microscopically, the coupling between the electric field of the propagating light and the electron spin in a magnetic medium occurs through the spin-orbit interaction splitting of optical absorption lines (Zeeman effect).

$$E_{SO} = \xi(r)\mathbf{S}\cdot\mathbf{L}$$

Here, $\xi(r)$ is the spin-orbit parameter or coupling constant, which depends on the gradient of the electrostatic potential of the nuclear charges.

Its values are of the order of **10-100meV** and, thus, the spin-orbit interaction is much weaker than the exchange interaction (≈ 1eV).

Electron theory of Magneto-Optics

Different electronic structure for up and down electrons

↓

Conductivity tensor of each layer

$$\overleftrightarrow{\sigma}(\vec{M}) = \begin{bmatrix} \sigma_0 & -\sigma_1 m_z & \sigma_1 m_y \\ \sigma_1 m_z & \sigma_0 & -\sigma_1 m_x \\ -\sigma_1 m_y & \sigma_1 m_x & \sigma_0 \end{bmatrix}$$

↓

Reflectivity matrix of whole sample

$$R = \begin{bmatrix} r_{ss} & r_{ps} \\ r_{sp} & r_{pp} \end{bmatrix}$$

↓

Measured Kerr effect

e.g.: $\theta_s = \Re\left(\frac{r_{ps}}{r_{ss}}\right)$

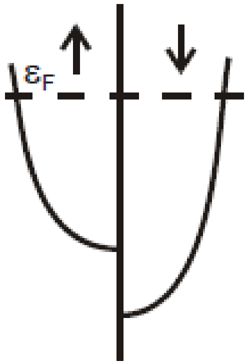

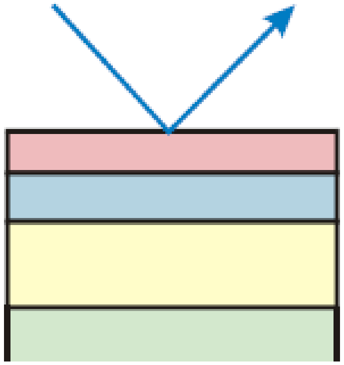

Microscopic origin of Magneto-Optics

Optical transitions between the d-orbitals and the p-orbitals

σ^+ and σ^- Selection rules $\Delta l = \pm 1, \quad \Delta m_l = \pm 1, \quad \Delta s = 0$

Only transition from m = ±1 to m = 0 are considered for simplicity

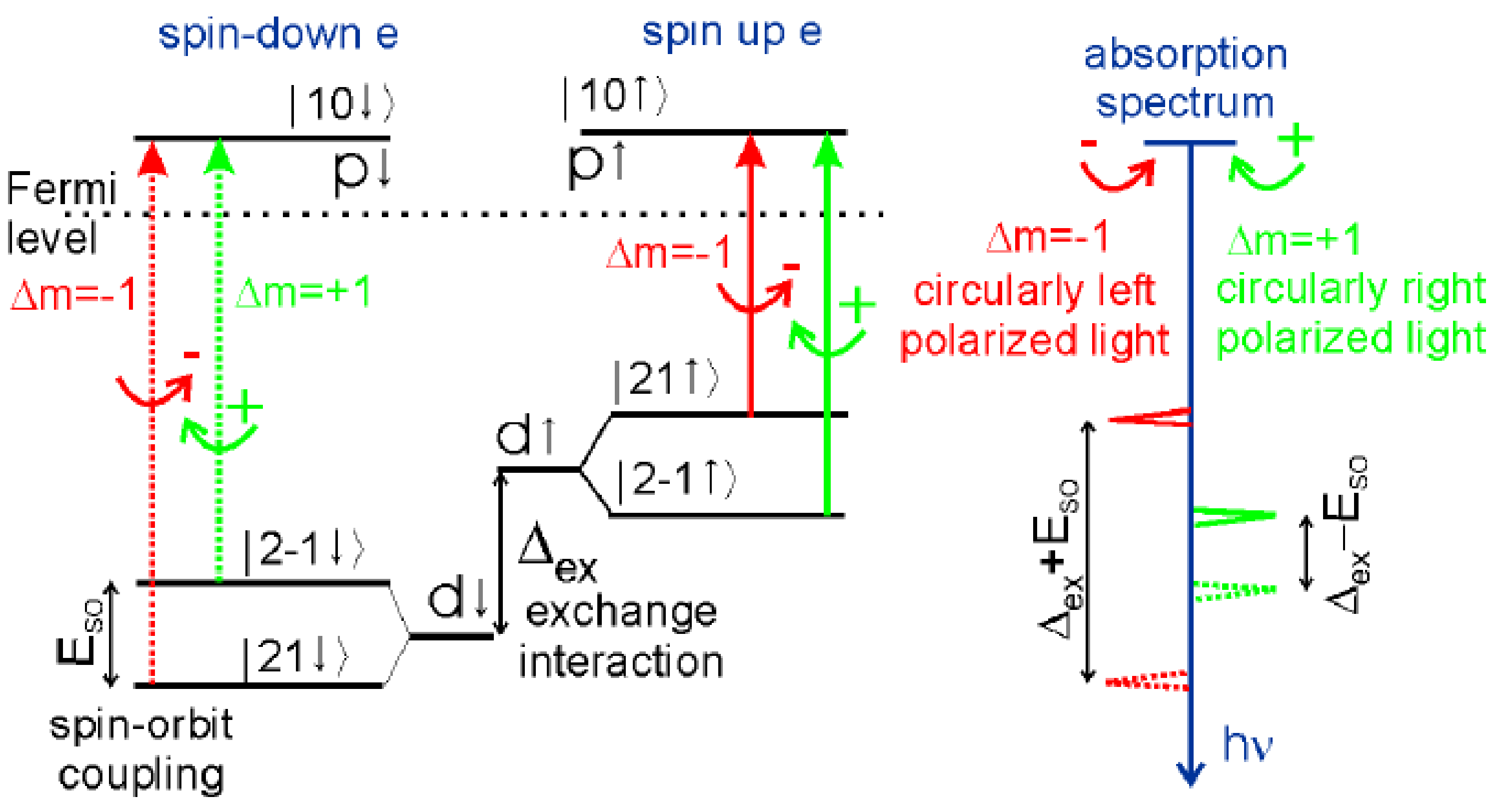

⇒ Both spin orbit coupling and exchange are necessary for MO activity

Microscopic origin of Magneto-Optics

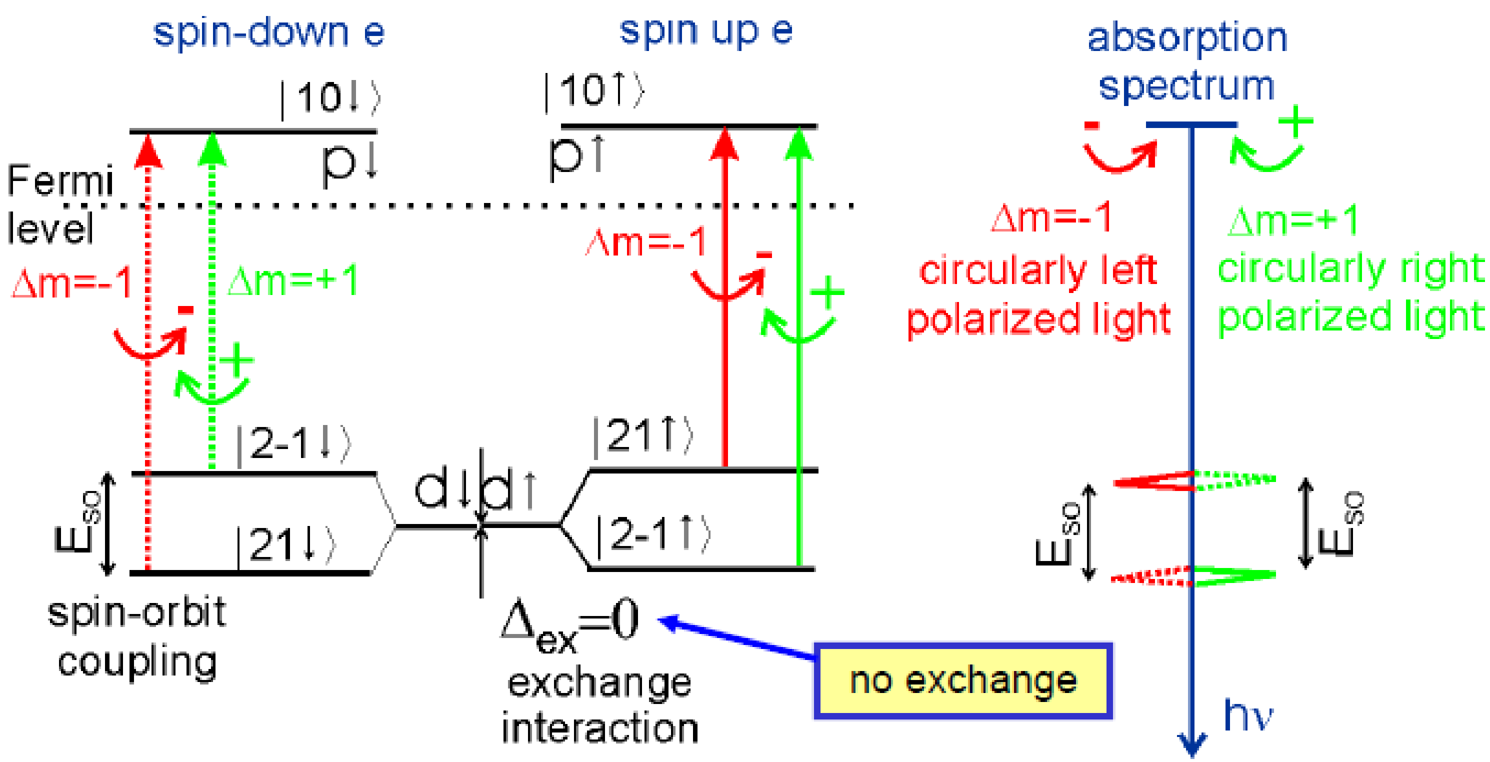

e.g. $\Delta_{ex}=0 \Rightarrow$ absorption spectra are the same $\Rightarrow$ no MO activity

Microscopic origin of Magneto-Optics

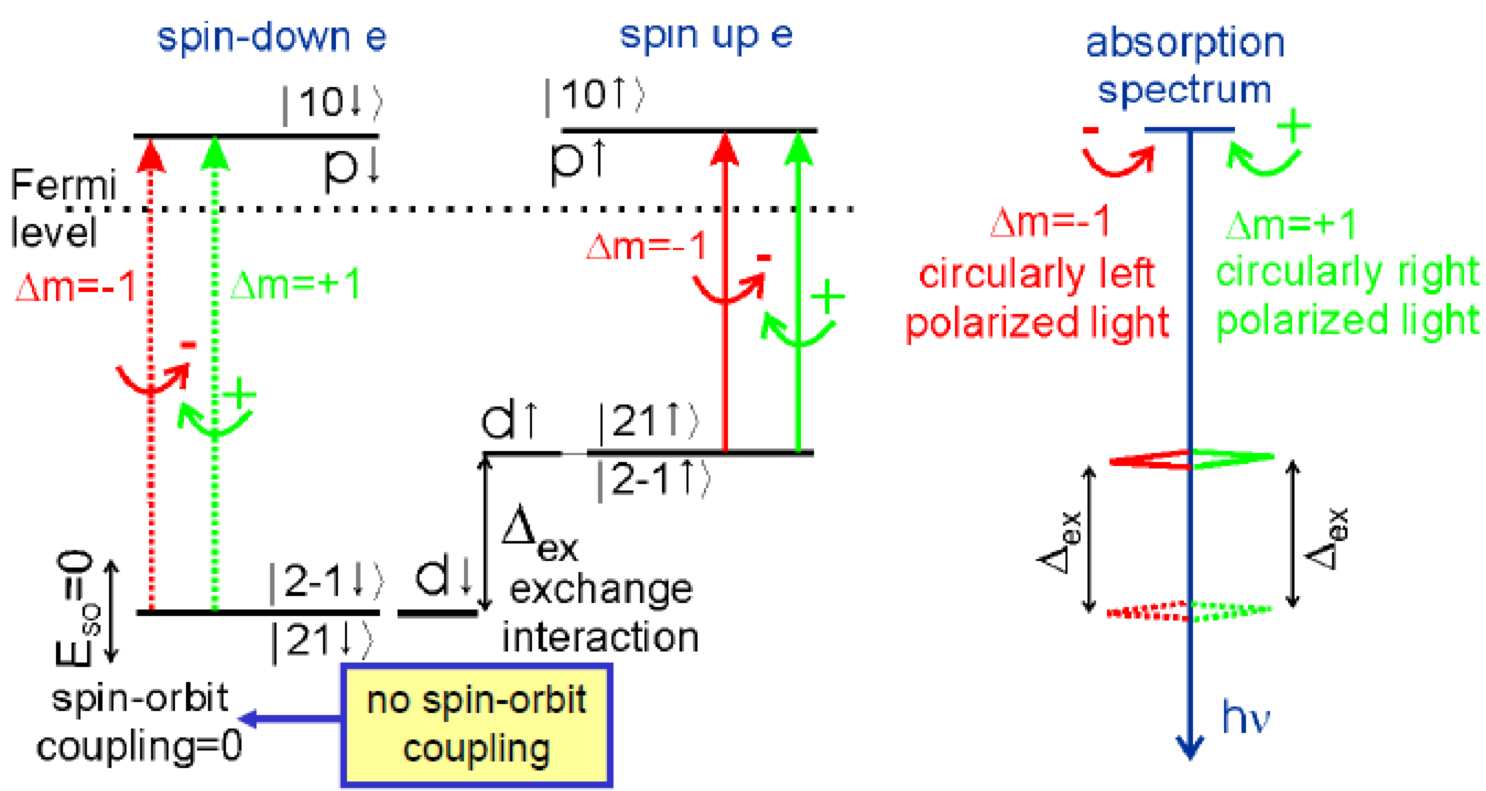

e.g. $E_{SO}=0$ ⇒ absorption spectra are the same ⇒ no MO activity

Microscopic origin of Magneto-Optics

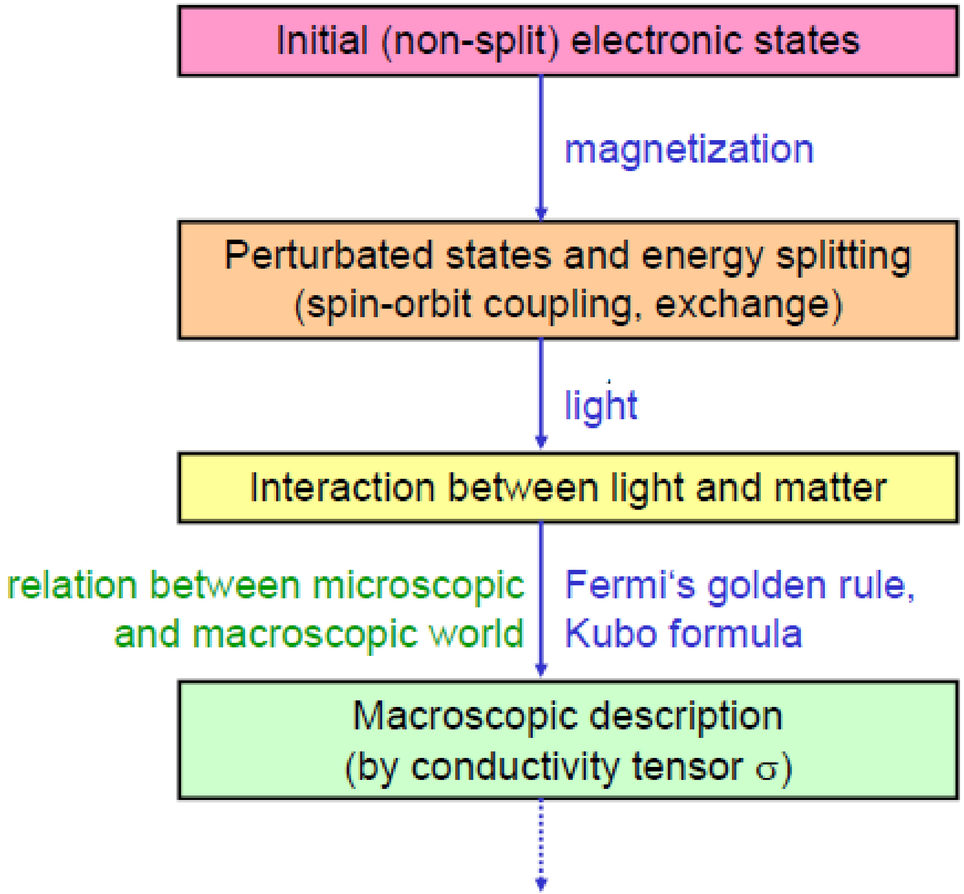

Microscopic origin of Magneto-Optics

⇒ Fermi's golden rule, Kubo formula:

(calculation of conductivity tensor)

- ⟨i|, |f⟩ - initial, final states
- $p_{\pm} = p_x \pm i p_y, \quad p_x = i\hbar \partial / \partial x$
  linear momentum operator

Diagonal conductivity:

$$\Re[\sigma_{xx}] \sim \sum_{i,f} f(E_i)\left[1 - f(E_f)\right] \times \left[|\langle i | p_- | f \rangle|^2 + |\langle i | p_+ | f \rangle|^2 \right] \times \delta\left(E_f - E_i - \hbar\omega\right)$$

Non-diagonal conductivity:

$$\Re[\sigma_{xy}] \sim \sum_{i,f} f(E_i)\left[1 - f(E_f)\right] \times \left[|\langle i | p_- | f \rangle|^2 - |\langle i | p_+ | f \rangle|^2 \right] \times \delta\left(E_f - E_i - \hbar\omega\right)$$

Sumation over all initial and final states in k-space

Occupancy of initial and final states (Fermi-Dirac distribution)

Transitions probabilities for left and right polarized light (non-zero only if selection rules are fulfilled)

Energy must be conserved

Bruno, PRB **53**, 9214 (1996)

Microscopic origin of Magneto-Optics

⇒ Selection rules of electric dipole transitions:

- Energy : $E_f - E_i = \hbar\omega$

  (absorbed photon energy = difference between final and initial state)

- Linear momentum : $\hbar\omega / c \approx 0$

  (photon has negligible linear momentum ⇒ vertical transitions)

- Electron spin : $\Delta s=0$

  (spin of electron is preserved for electric dipole transitions)

- Orbitum momentum : $\Delta l=\pm 1$

  (photon has angular momentum 1ħ). Therefore only s↔p, p↔d etc. are allowed

- Orbital momentum along z-axis : $\Delta m=\pm 1$

  (determines if photon is right/left polarized)

$$\langle i \mid p_+ \mid f \rangle \neq 0$$

- ⟨i|, |f⟩ - initial, final states
- $p_{\pm} = p_x \pm i p_y, \quad p_x = i\hbar \partial / \partial x$ linear momentum operator

Electron theory of Magneto-Optics

MOKE results from a lifting of orbital degeneracy due to spin-orbit interaction (SOI) in the presence of spontaneous spin polarization.

- Magnetization→Splitting of spin-states (Exchange)
  - No direct cause of difference of optical response between LCP and RCP
- Spin-orbit interaction→Splitting of orbital states
  - Absorption of circular polarization→Induction of circular motion of electrons
- Condition for large magneto-optical response
  - Presence of strong (allowed) transitions
  - Involving elements with large spin-orbit interaction
  - Not directly related with Magnetization

A simple case: M || z

$$\tilde{\varepsilon} = \begin{pmatrix} \varepsilon_{xx} & \varepsilon_{xy} & 0 \\ -\varepsilon_{xy} & \varepsilon_{xx} & 0 \\ 0 & 0 & \varepsilon_{xx} \end{pmatrix}$$

$\varepsilon_{xy} = i\varepsilon_0 Q\, m_z;$

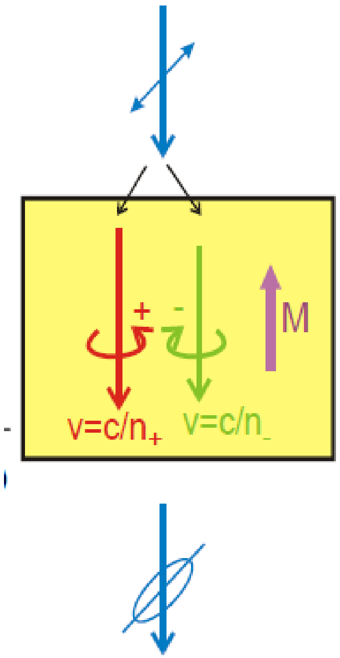

Maxwell Equation $$rot\,rot\,E(\omega) + \frac{\tilde{\varepsilon}(\omega)}{c^2}\frac{\partial^2}{\partial t^2}E(\omega) = 0$$

$$E(\omega) = E_0 e^{i(nk_0 z - \omega t)} \Rightarrow n^2\mathbf{E} - \mathbf{n}(\mathbf{n}\cdot\mathbf{E}) - \hat{\varepsilon}\mathbf{E} = 0$$

Eigenequation $$\begin{pmatrix} n^2 - \varepsilon_{xx} & -\varepsilon_{xy} & 0 \\ \varepsilon_{xy} & n^2 - \varepsilon_{xx} & 0 \\ 0 & 0 & -\varepsilon_{zz} \end{pmatrix}\begin{pmatrix} E_x \\ E_y \\ E_z \end{pmatrix} = 0$$

Eigenvalue $n_\pm^2 = \varepsilon_{xx} \pm i\varepsilon_{xy}$ ➡ Eigenmodes: LCP and RCP

Different modes :different speed and attenuation

Without off-diagonal terms: No difference between LCP & RCP

Therefore, incident light becomes elliptically polarized after propagation in a MO active material

Phenomenology of MO effect

Linearly polarized light can be decomposed to LCP and RCP

Difference in phase causes rotation of the direction of Linear polarization

Different speed (phase lag)

Difference in amplitudes makes Elliptically polarized light

Different attenuation

In general, elliptically polarized light With the principal axis rotated

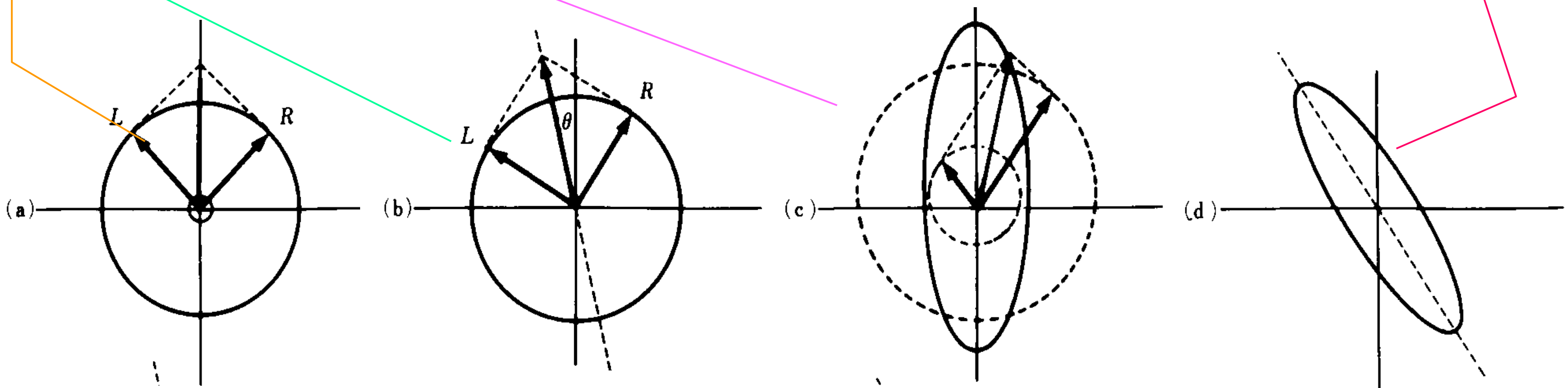

General case: Oblique incidence and arbitrary direction of M

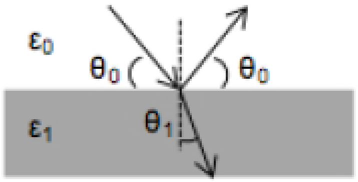

$$\begin{pmatrix} r_{pp} & r_{ps} \\ r_{sp} & r_{ss} \end{pmatrix} \Rightarrow$$

$$r_{pp} = \frac{n_1\cos\theta_0 - n_0\cos\theta_1}{n_1\cos\theta_0 + n_0\cos\theta_1} - \frac{2n_0 n_1^{-1}\cos\theta_0\sin\theta_1\epsilon_{xz}}{(n_1\cos\theta_0 + n_0\cos\theta_1)^2}$$

$$r_{sp} = \frac{-n_0 n_1^{-1}\cos\theta_0(\epsilon_{xy}\cos\theta_1 + \epsilon_{yz}\sin\theta_1)}{(n_1\cos\theta_0 + n_0\cos\theta_1)(n_0\cos\theta_0 + n_1\cos\theta_1)\cos\theta_1}$$

$$r_{ps} = \frac{-n_0 n_1^{-1}\cos\theta_0(\epsilon_{xy}\cos\theta_1 - \epsilon_{yz}\sin\theta_1)}{(n_1\cos\theta_0 + n_0\cos\theta_1)(n_0\cos\theta_0 + n_1\cos\theta_1)\cos\theta_1}$$

$$r_{ss} = \frac{n_0\cos\theta_0 - n_1\cos\theta_1}{n_0\cos\theta_0 + n_1\cos\theta_1}$$

$$n_i = \sqrt{\epsilon_i} \qquad \cos\theta_1 = \sqrt{1-\sin^2\theta_1} = \sqrt{1-\frac{n_0^2}{n_1^2}\sin^2\theta} = \frac{\sqrt{n_1^2 - n_0^2\sin^2\theta}}{n_1}$$

$\varepsilon_{xy} = i\varepsilon_1 Q\, m_z$; $\varepsilon_{xz} = -i\varepsilon_1 Q\, m_y$; $\varepsilon_{yz} = i\varepsilon_1 Q\, m_x$;

$\varepsilon_{xy} = -\varepsilon_{yx}$; $\varepsilon_{zx} = -\varepsilon_{xz}$; $\varepsilon_{zy} = -\varepsilon_{yz}$;

$\Rightarrow$

$\mathbf{r_{pp} = r^0_{pp} + r_{pp}^M \propto m_y}$

$\mathbf{r_{ps} \propto - m_x - m_z}$

$\mathbf{r_{sp} \propto m_x - m_z}$

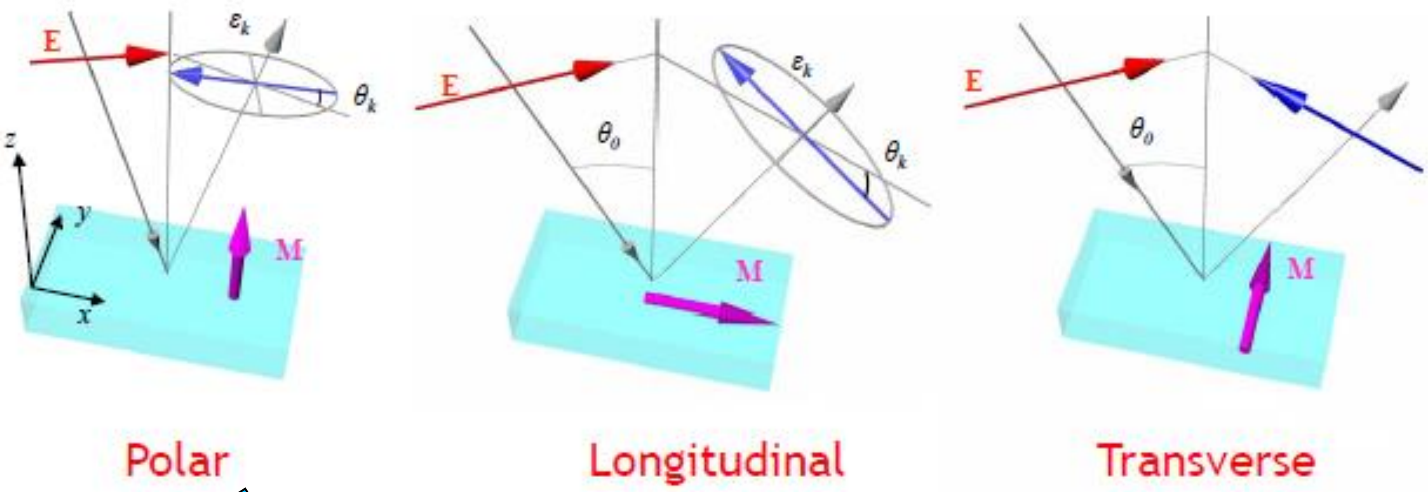

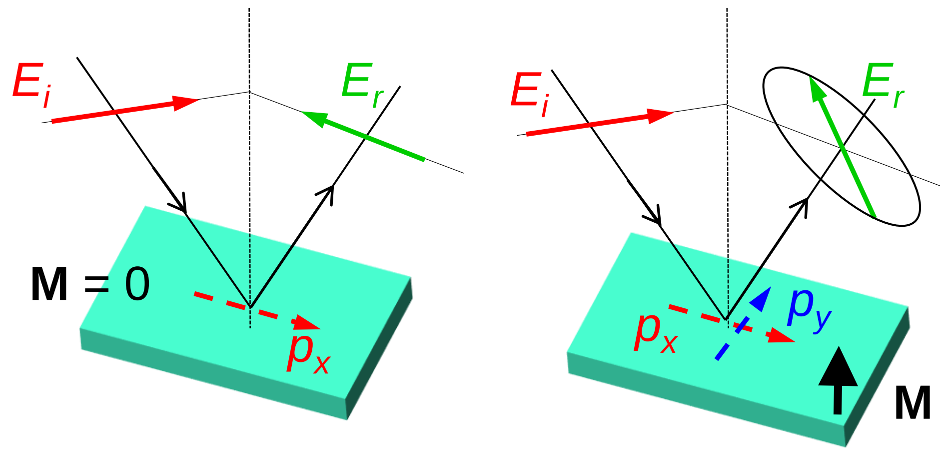

Polarization conversion

$$p_y = \frac{\varepsilon_{yx}}{(\varepsilon_{xx} - \varepsilon_0)}$$

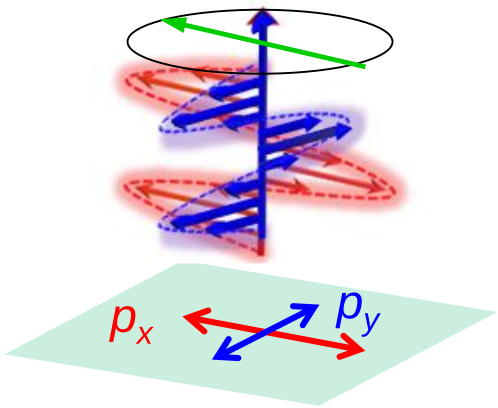

Longitudinal and polar Kerr effect

Normalized representation

Elliptically polarized light

$$\tilde{E}_r = \begin{bmatrix} r_{pp} \\ r_{sp} \end{bmatrix} = \begin{bmatrix} 1 \\ \frac{|r_{sp}|}{|r_{pp}|} e^{i\delta} \end{bmatrix} = \begin{bmatrix} 1 \\ \frac{|r_{sp}|}{|r_{pp}|}(\cos\delta + i\sin\delta) \end{bmatrix}$$

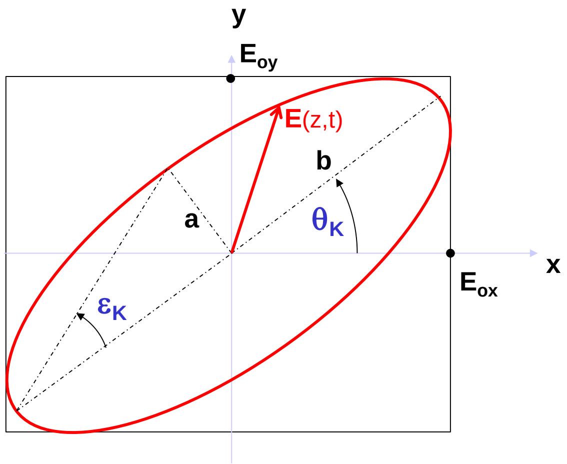

$$\tan 2\theta_K = \frac{2|r_{pp}||r_{sp}|\cos\delta}{|r_{pp}|^2 - |r_{sp}|^2} = \frac{2b\cos\delta}{1-b^2}$$

$$\sin 2\varepsilon_K = \frac{2|r_{pp}||r_{sp}|\sin\delta}{|r_{pp}|^2 + |r_{sp}|^2} = \frac{2b\sin\delta}{1+b^2}$$

$r_{sp} << r_{pp}$

$$\tan 2\theta_K \approx 2\theta_K \approx \frac{2|r_{sp}|\cos\delta}{|r_{pp}|}$$

$$\sin 2\varepsilon_K \approx 2\varepsilon_K \approx \frac{2|r_{sp}|\sin\delta}{|r_{pp}|}$$

$$\mathrm{Re}\left[\frac{r_{sp}}{r_{pp}}\right] = \frac{|r_{sp}|}{|r_{pp}|}\cos\delta \qquad \mathrm{Im}\left[\frac{r_{sp}}{r_{pp}}\right] = \frac{|r_{sp}|}{|r_{pp}|}\sin\delta$$

θ_K $\mathrm{Re}\left[\frac{r_{sp}}{r_{pp}}\right]$ $\mathrm{Re}\left[\frac{r_{ps}}{r_{ss}}\right]$ ε_K $\mathrm{Im}\left[\frac{r_{sp}}{r_{pp}}\right]$ $\mathrm{Im}\left[\frac{r_{ps}}{r_{ss}}\right]$

Measurement of ellipticity

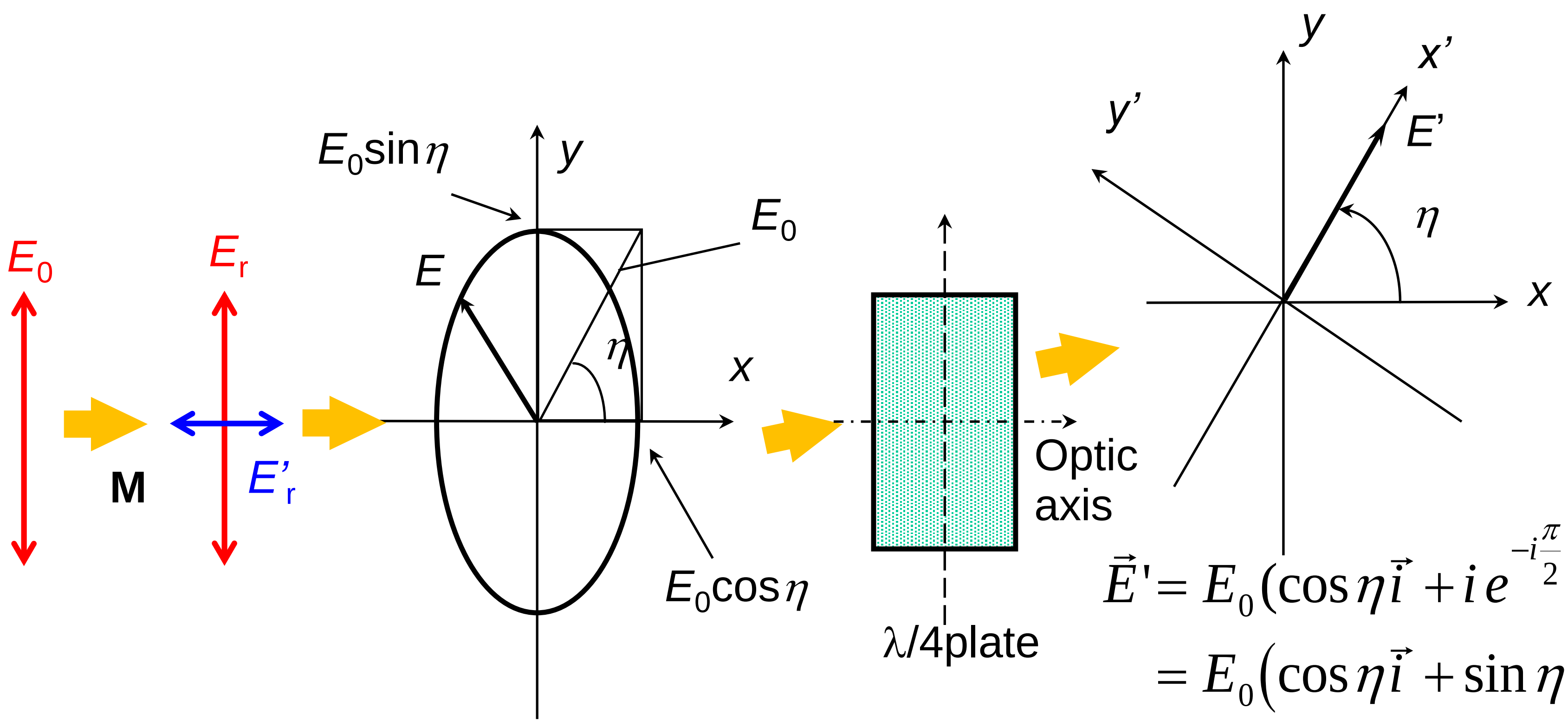

$$\vec{E} = E_0(\cos\eta\,\vec{i} + i\sin\eta\,\vec{j})$$

$$\vec{E}' = E_0(\cos\eta\,\vec{i} + i\,e^{-i\frac{\pi}{2}}\sin\eta\,\vec{j})$$
$$= E_0(\cos\eta\,\vec{i} + \sin\eta\,\vec{j})$$
$$= E_0\,\vec{i}\,'$$

Measurement of ellipticity & rotation: high sensitivity

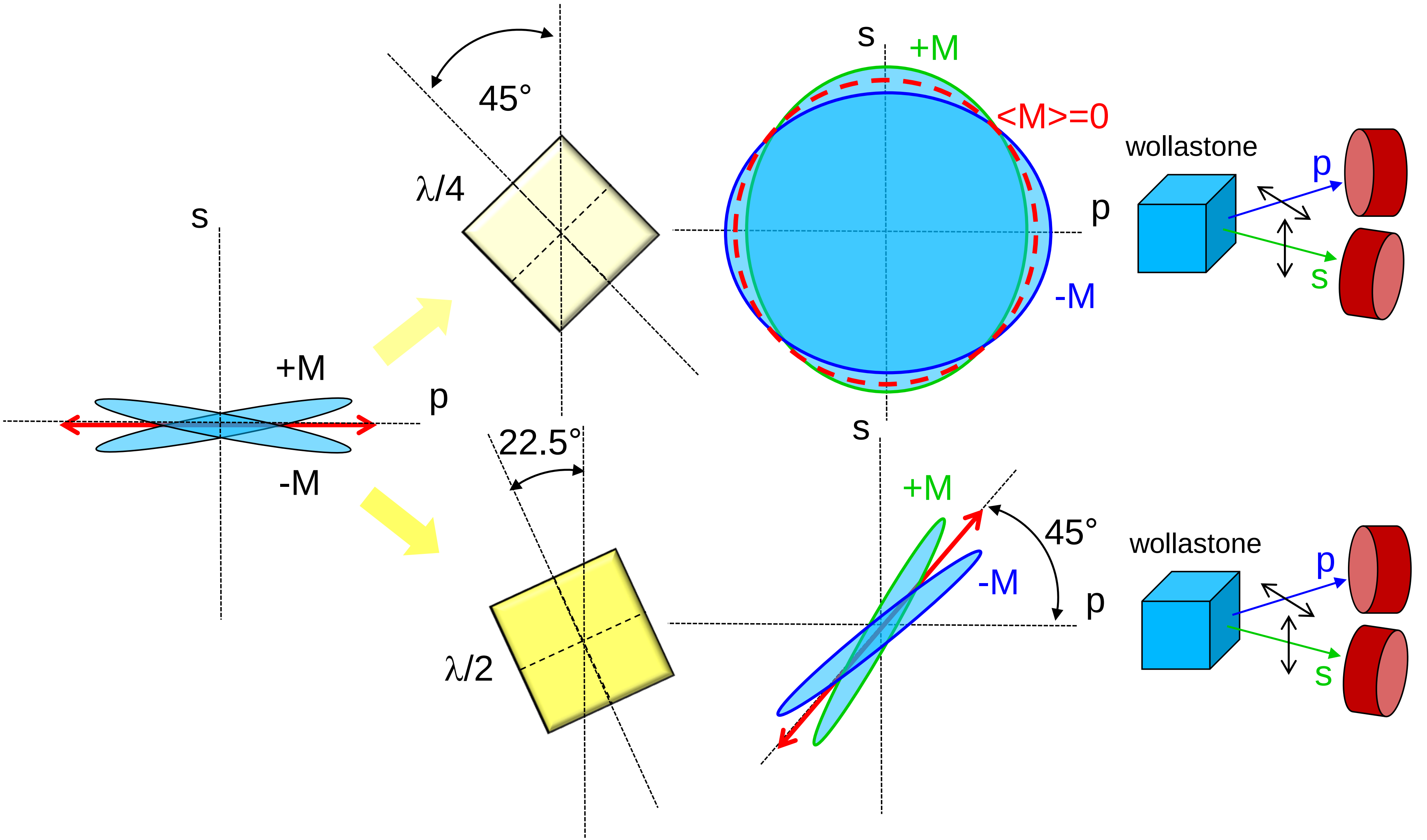

Measurement of ellipticity & rotation: high sensitivity

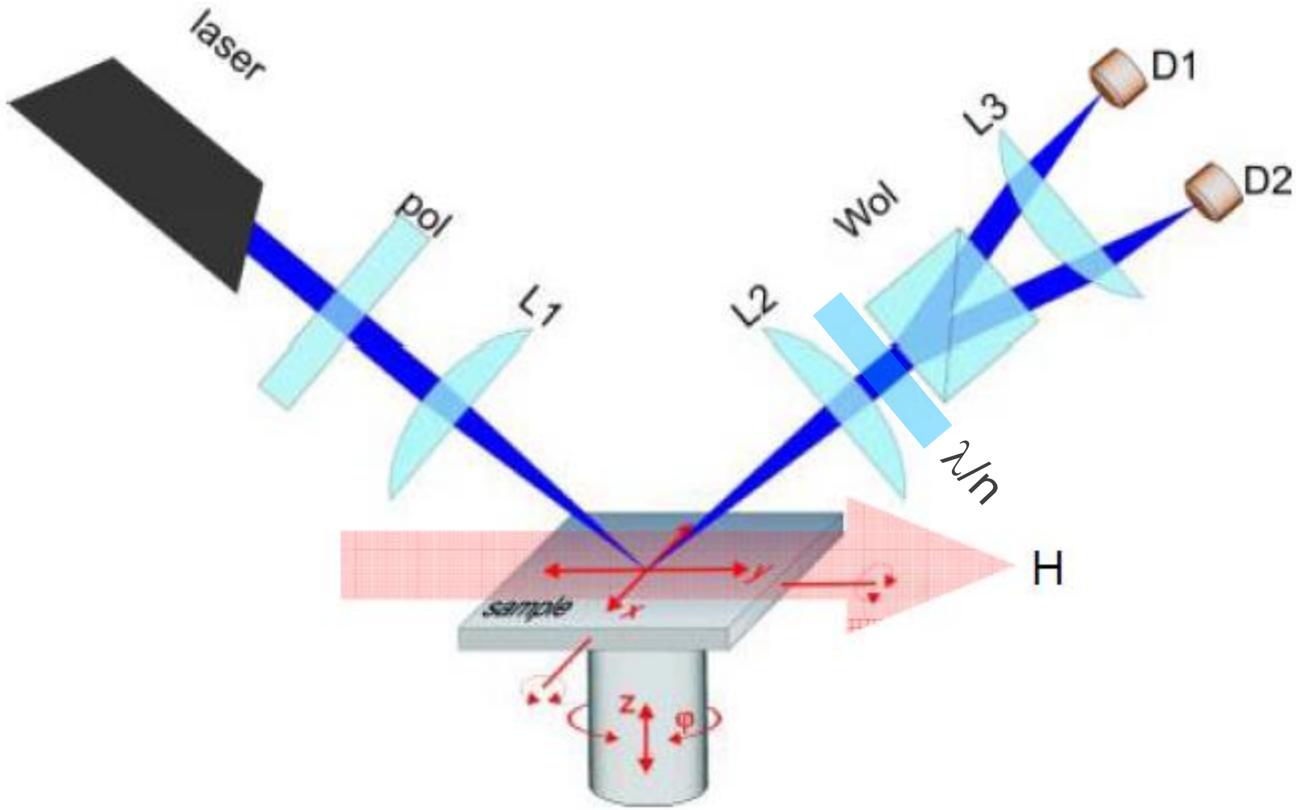

Measuring θ_K and ε_K

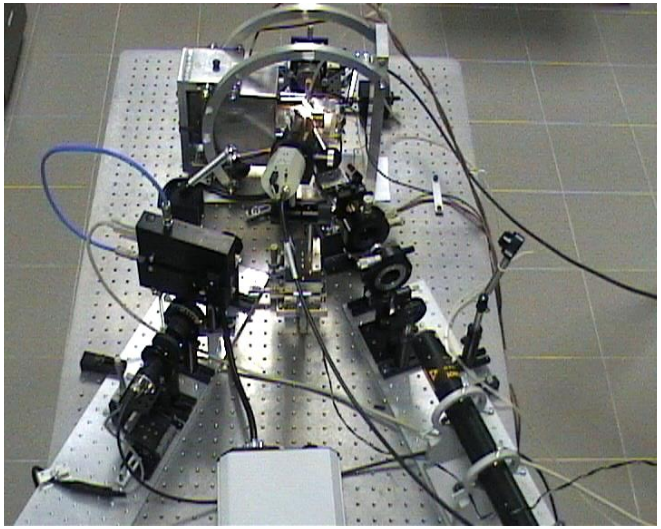

Modulation polarization technique for recording the longitudinal and polar Kerr effects, which are proportional to the magnetization components m_x m_z..

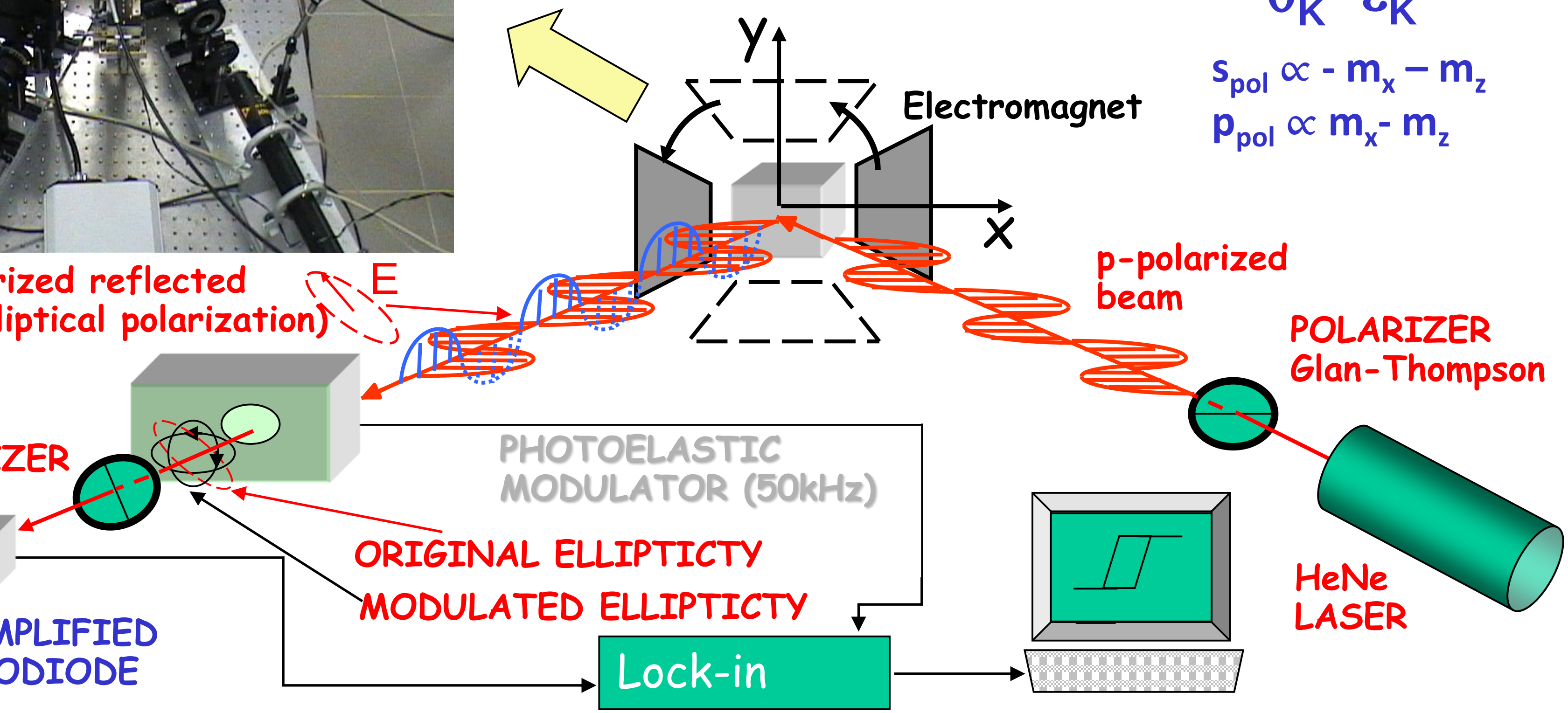

More details in: P. Vavassori, Appl. Phys. Lett. **77**, 1605 (2000)

Transverse Kerr effect

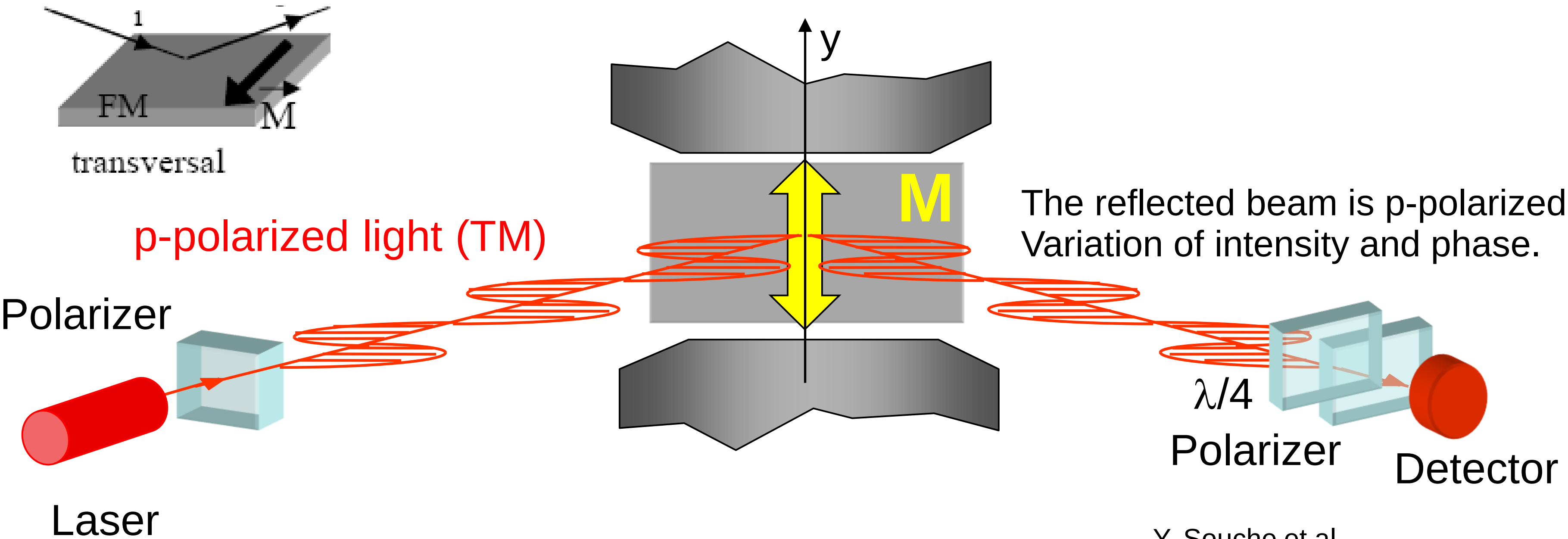

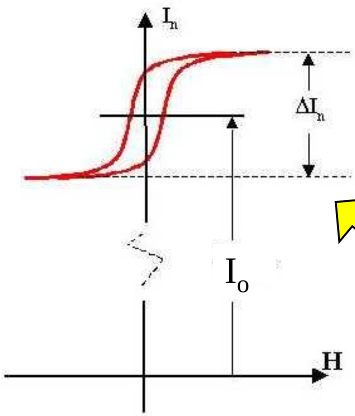

$$E_r = r_{pp} E_o$$

$$r_{pp} = r^o_{pp} + r^m_{pp} m_y$$

$$I_r = E_r (E_r)^*$$

$$I_r = I_o + \Delta I_m \qquad \Delta I_m / I_o \; \alpha \; m_y$$

Y. Souche et al.
JMMM 226-230, 1686 (2001);
JMMM 242-245, 964 (2002).

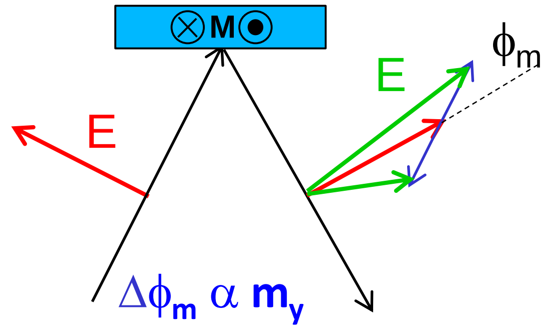

Examples of application of MOKE for magnetic characterization of materials and nanosctructures

Vector analysis of reversal

Reconstruction of the magnetization vector during the reversal

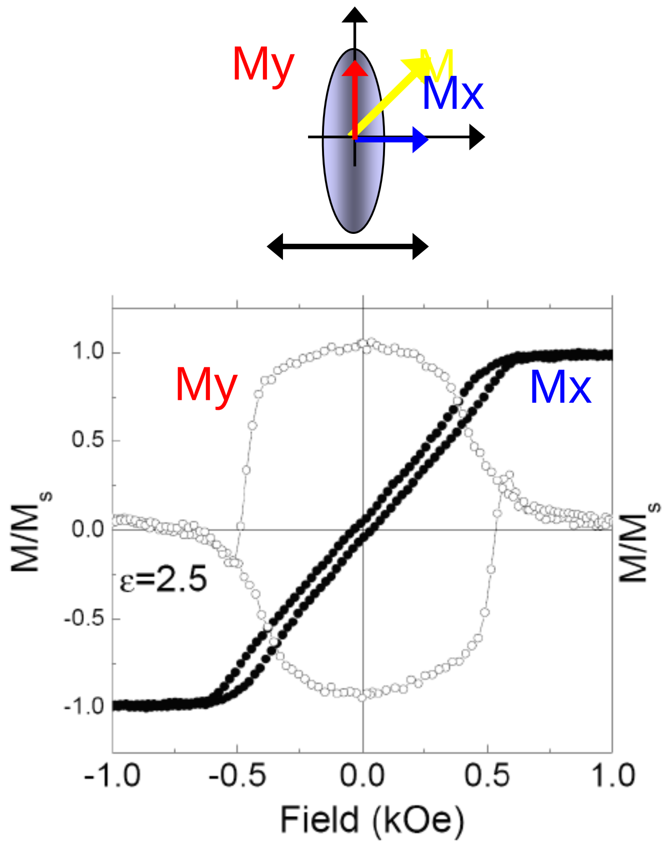

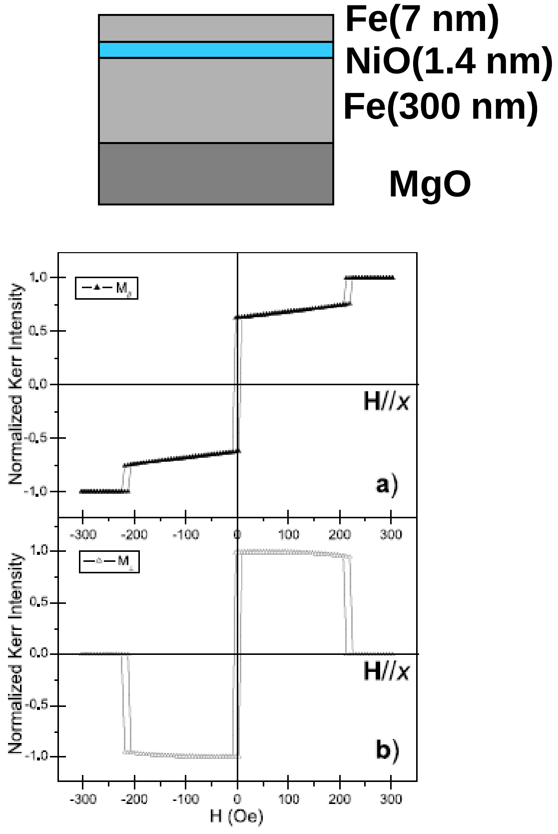

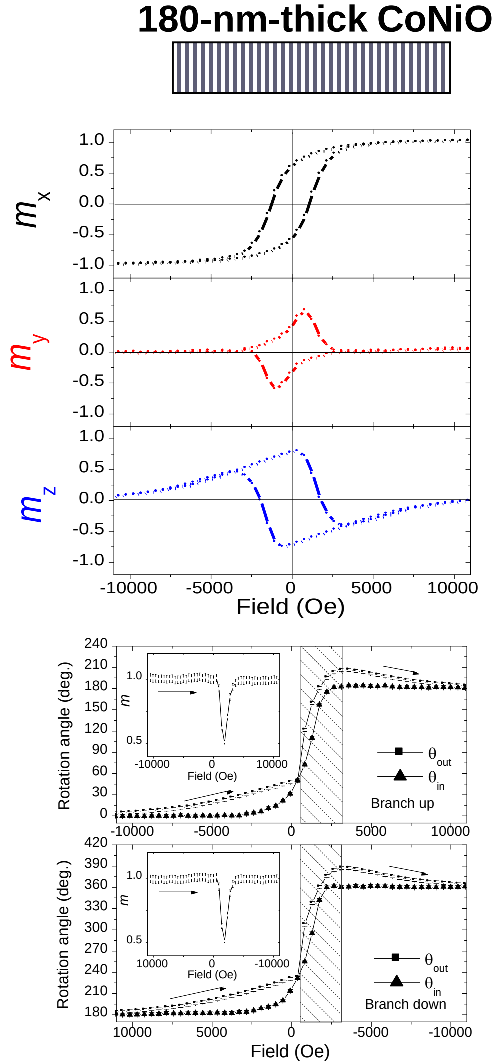

- F. Carace, P. Vavassori, G. Gubbiotti, S. Tacchi, M. Madami, G. Carlotti, and T. Okuno, Thin Solid Films **515/2**, 727 (2006).
- A. Brambilla, P. Biagioni, M. Portalupi, P. Vavassori, M. Zani, M. Finazzi, R. Bertacco, L. Duò, and F. Ciccacci, Phys. Rev. B. **72**, 174402 (2005).
- P. Vavassori, Appl. Phys. Lett. 77, 1605 (2000) .

Element sensitivity (and layer sensitivity)

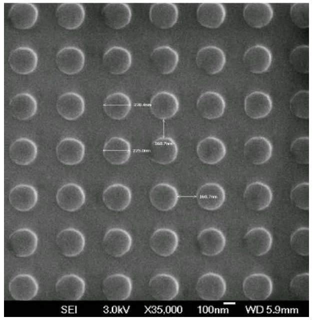

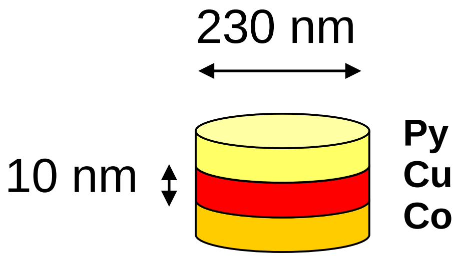

XMCD x-ray magnetic circular dichroism (FeL3 Py hysteresis loop and CoL3 thresholds), → chemical and magnetic sensitivity

MOKE

XMCD

Simulations

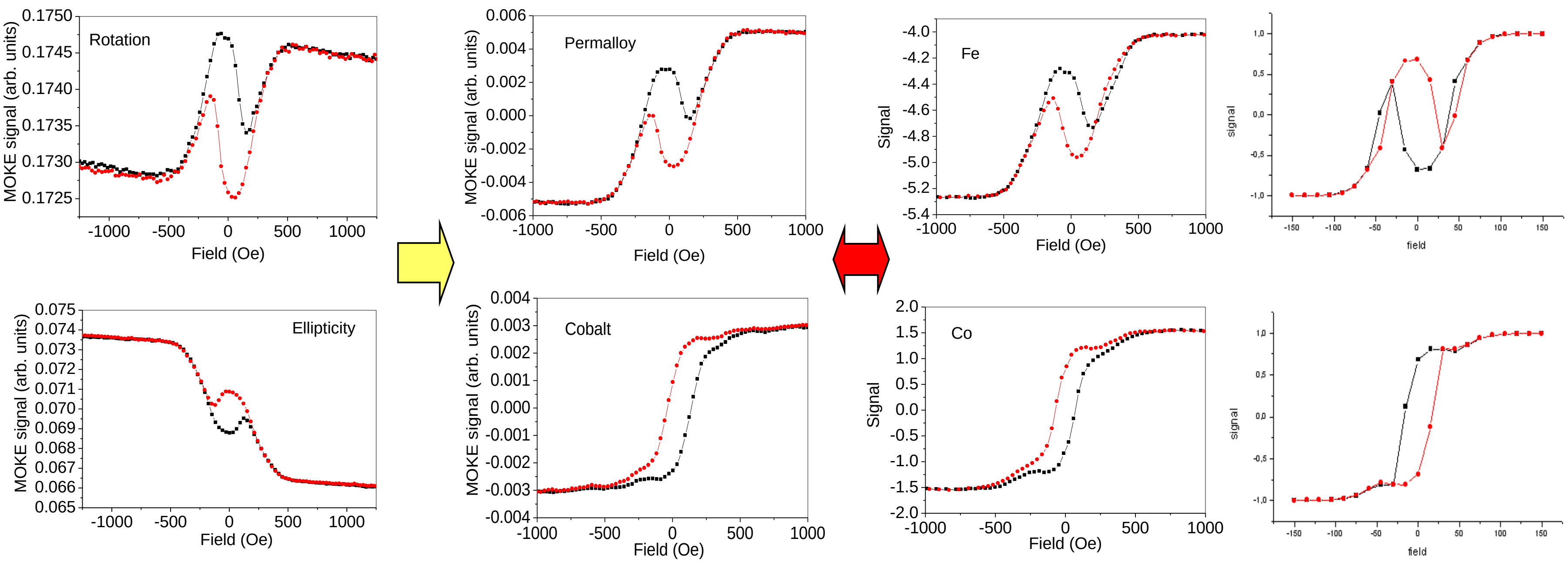

JOURNAL OF PHYSICS D-APPLIED PHYSICS 41, 134014 (2008)

Element sensitivity (thin layer regime)

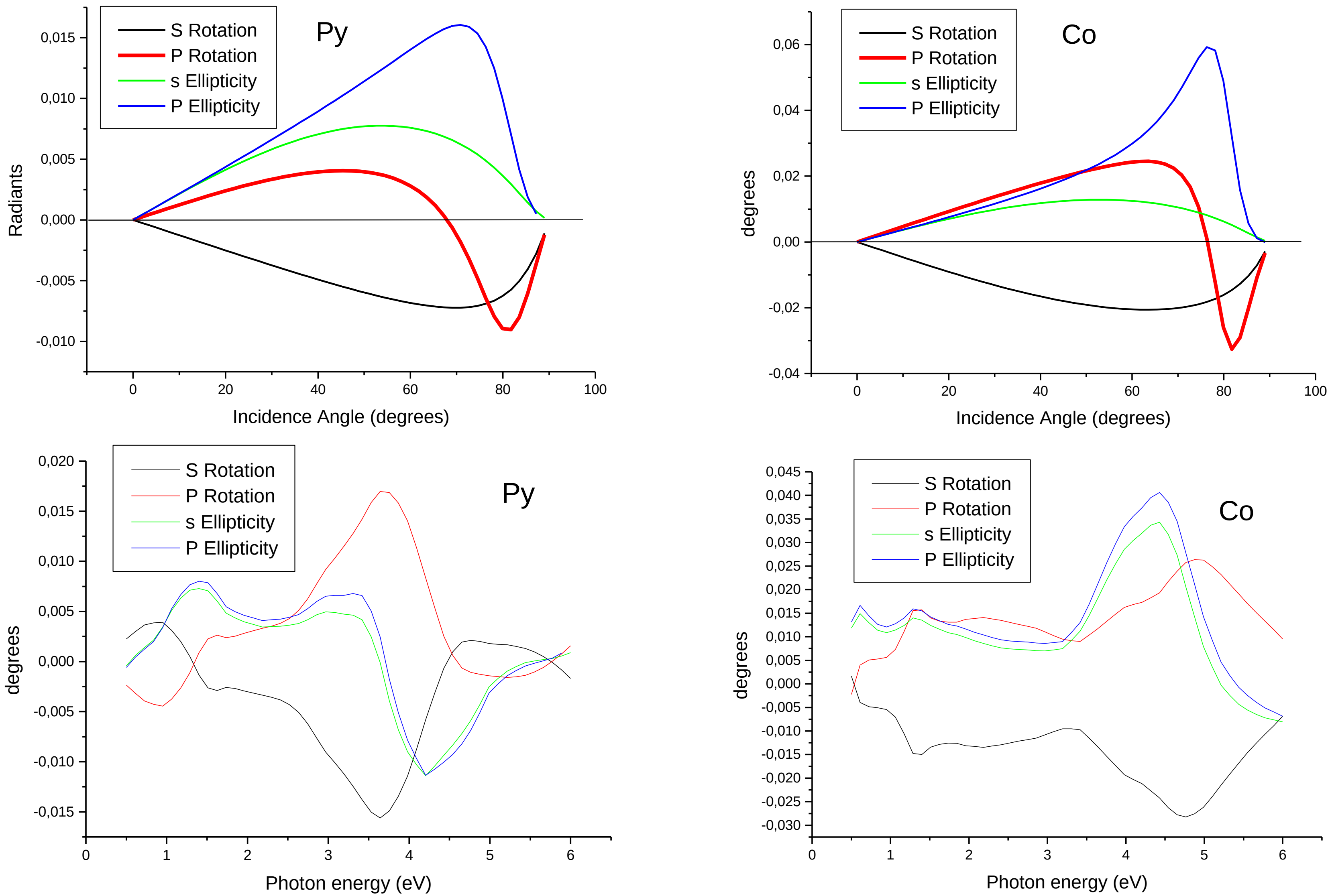

Layer sensitivity

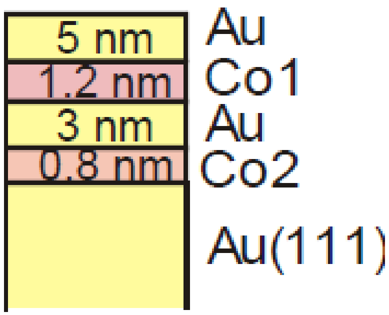

Measured MOKE is:

$$\theta_s = \Re\left(\frac{r_{ps}}{r_{ss}}\right)$$

When Babinet-Soleil compensator of retardation ψ added between sample and detector:

$$\theta_s = \Re\left(\frac{r_{ps}}{r_{ss}} e^{i\psi}\right) \Rightarrow$$

ψ =0°

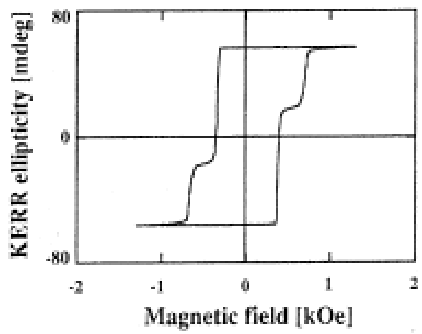

ψ = -41°

Co2 magnetization

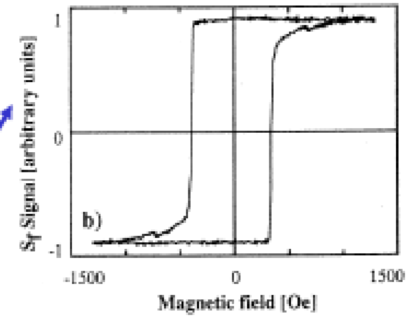

ψ = -46.7°

Co1 magnetization

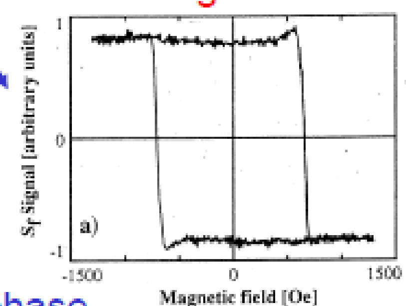

As Co1 and Co2 have different phase, different ψ may provide sensitivity solely to Co1 or Co2 layers

MOKE transverse susceptibility: anisotropy

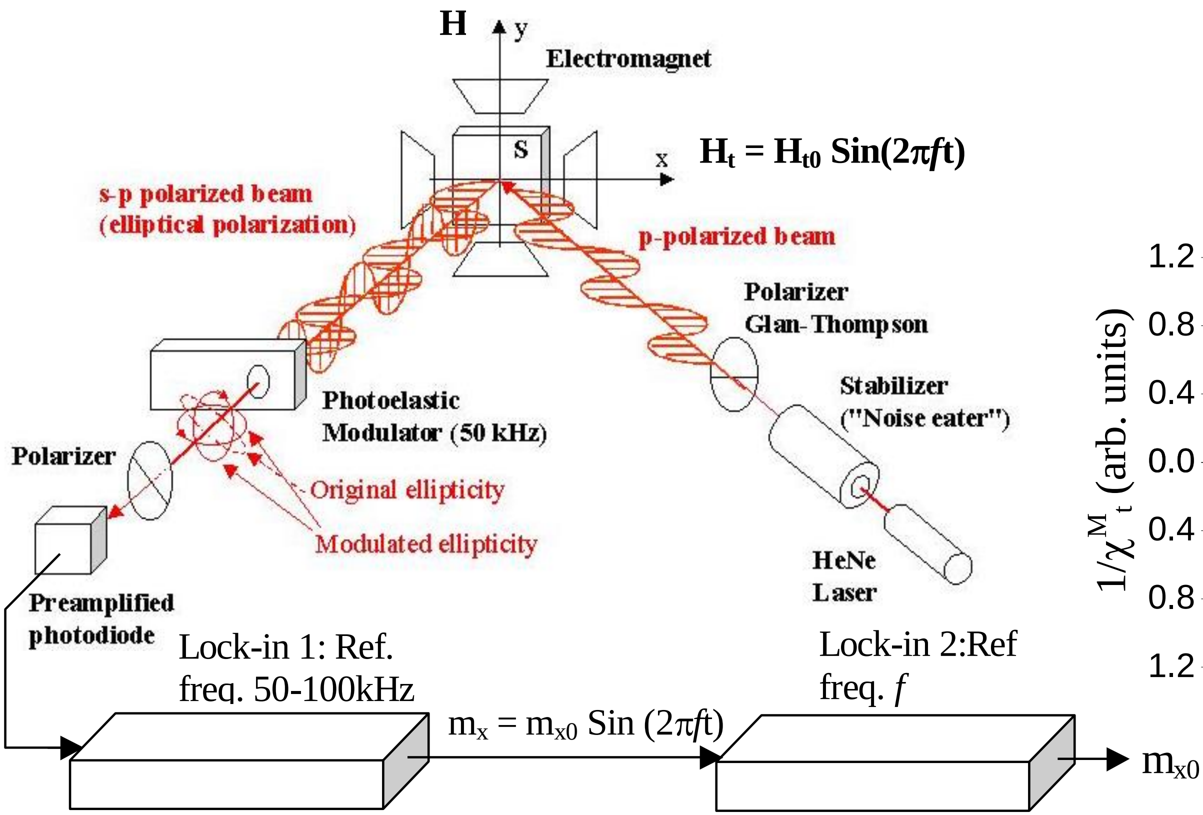

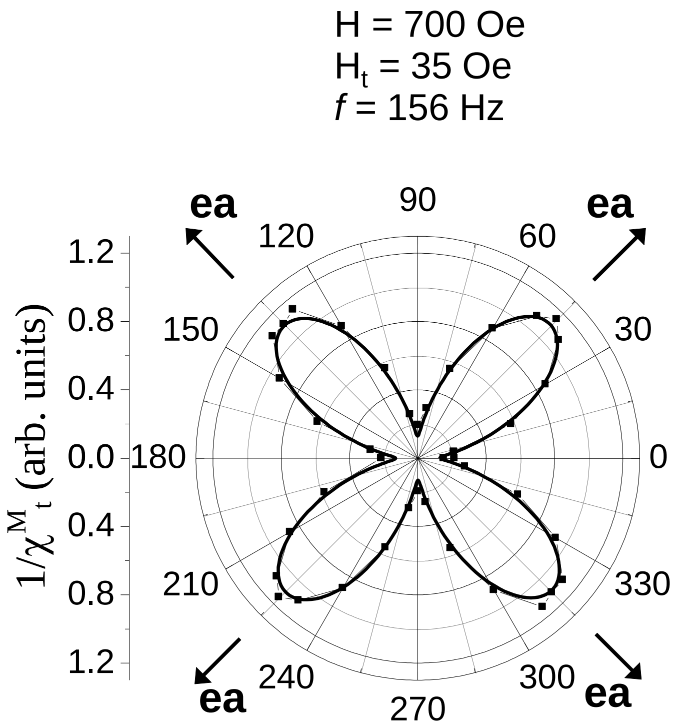

The quantity measured with the Lock-in2 is proportional to the transverse suceptibility $\chi_t = \Delta\theta_0 / H_{t0}$.

It can be shown that **: $1/\chi_t = (E_o''(\theta_{eq}) / \langle M\rangle_{eq})$** where **$E_o(\theta_{eq})$** is the total free energy and $\langle M\rangle_{eq}$ is the average magnetization, which makes an angle θ_{eq} with the EA.

Configurational anisotropy

Even small perturbations from uniform magnetization which must exist in any nonellipsoidal magnet give rise to a (strong) angular dependence of magnetostatic dipolar energy in symmetric squared particles, which should be magnetically isotropic in the approximation of M uniform. This anisotropy is called *<u>configurational anisotropy</u>*

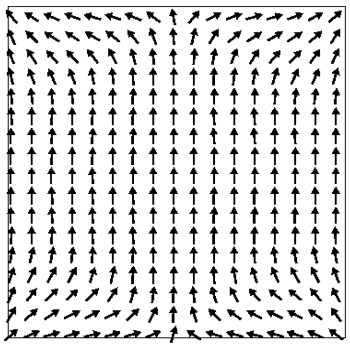

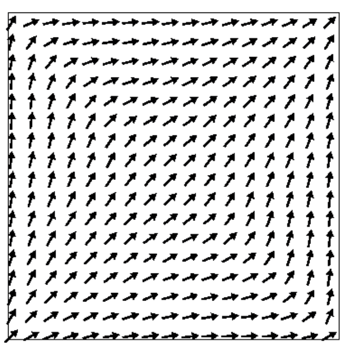

Py squares
150 x 150 x 15 nm^3

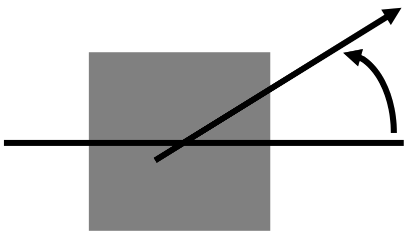

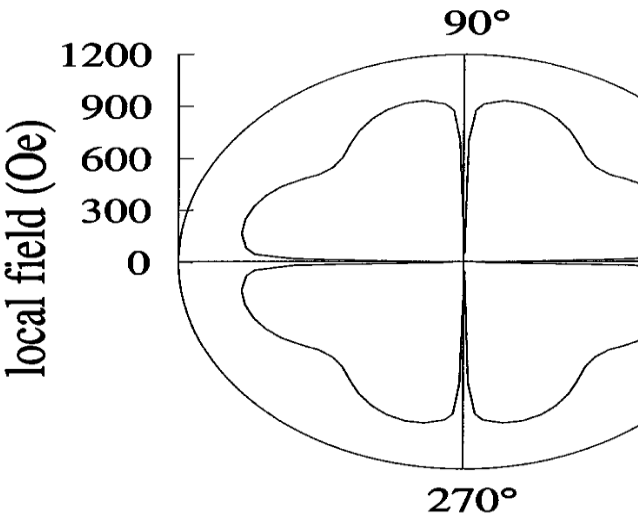

fourfold symmetry
eightfold symmetry

P. Vavassori, et al., Phys. Rev. B **72**, 054405 (2005)

Kerr microscopy: focused laser beam

Micro-MOKE

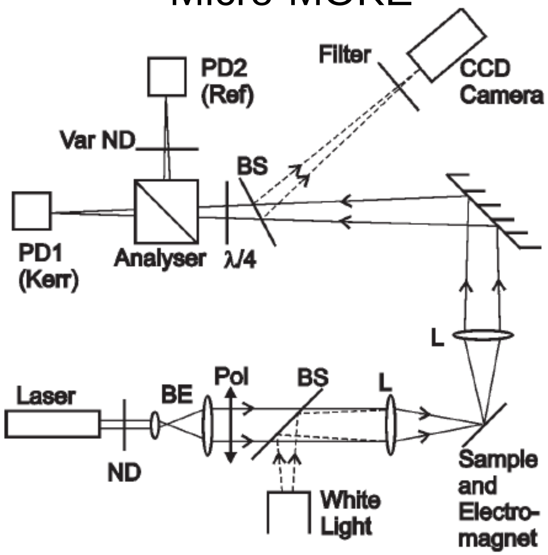

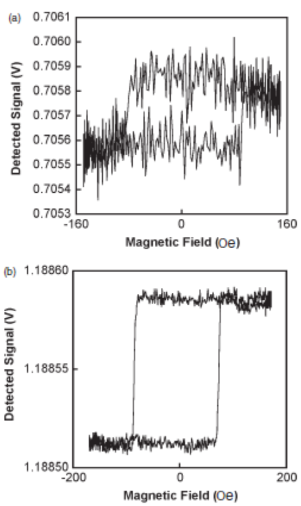

Py wire 200 nm wide
Single loop

Py wire 100 nm wide
1000 loops

D. A. Allwood, et al., J. Phys. D: Appl. Phys. 36, 2175 (2003)

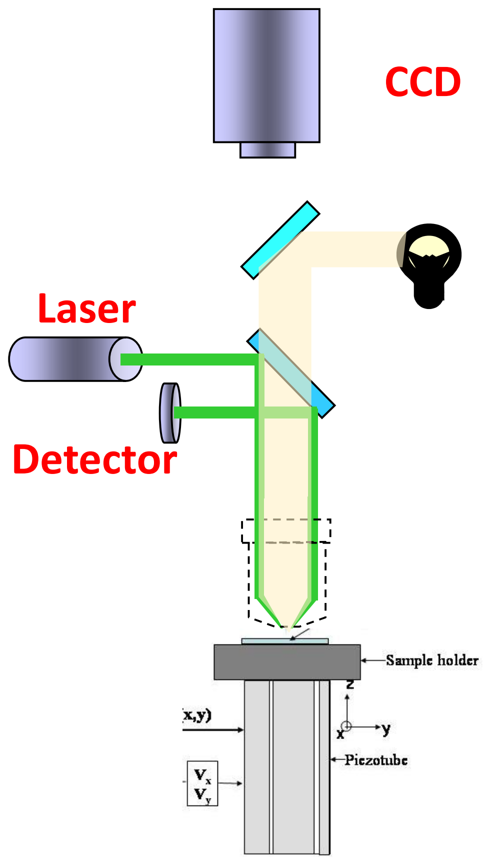

Py wires 175 nm wide

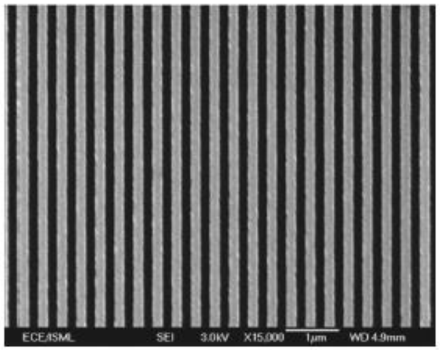

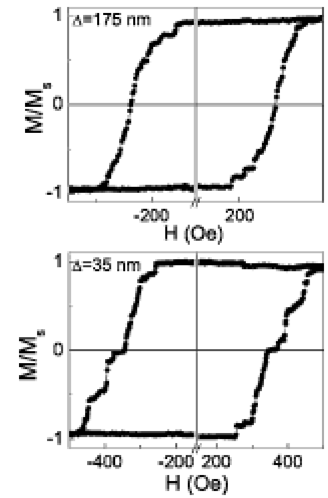

PHYSICAL REVIEW 72, 224413 (2005)

Kerr microscopy: imaging

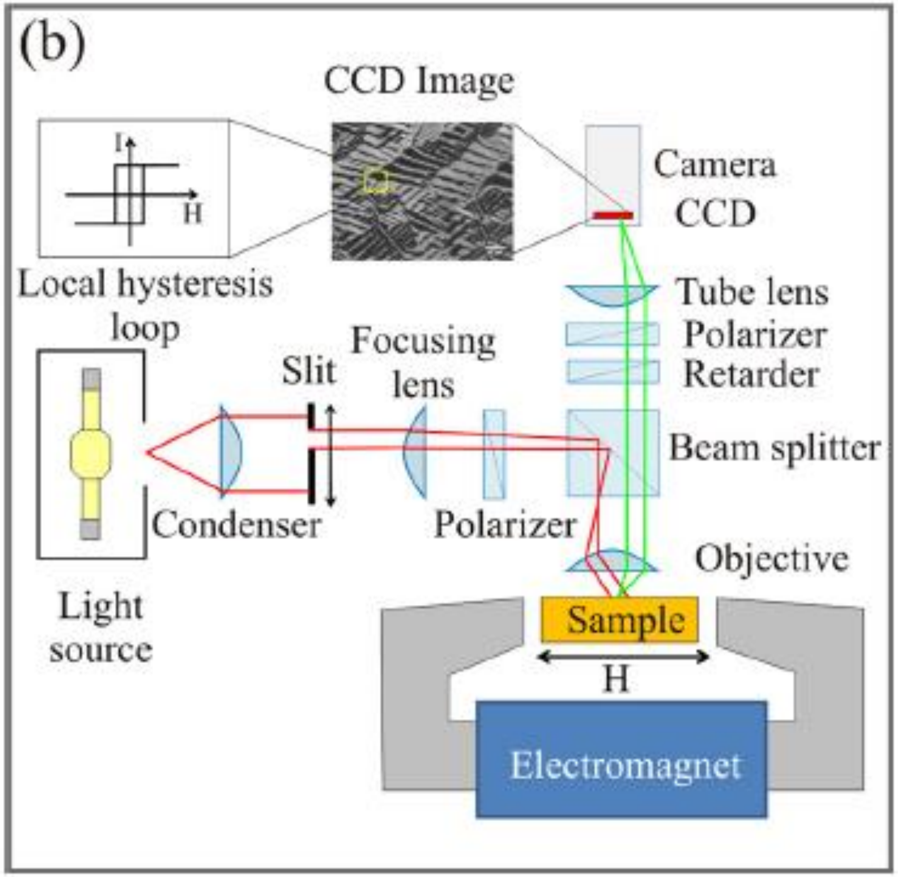

Longitudinal and transverse

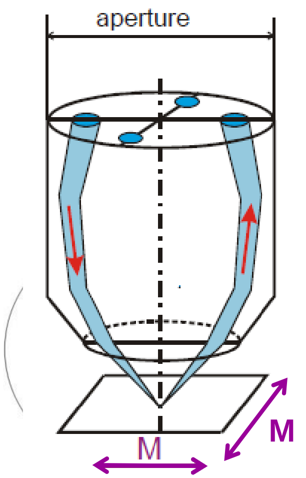

Polar

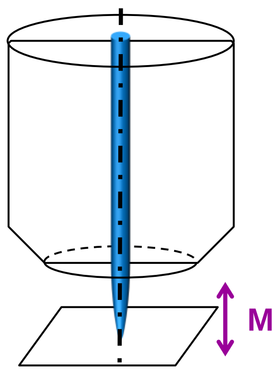

Magnetometry of ultra-small nanostructure

EBID
electron beam induced deposition

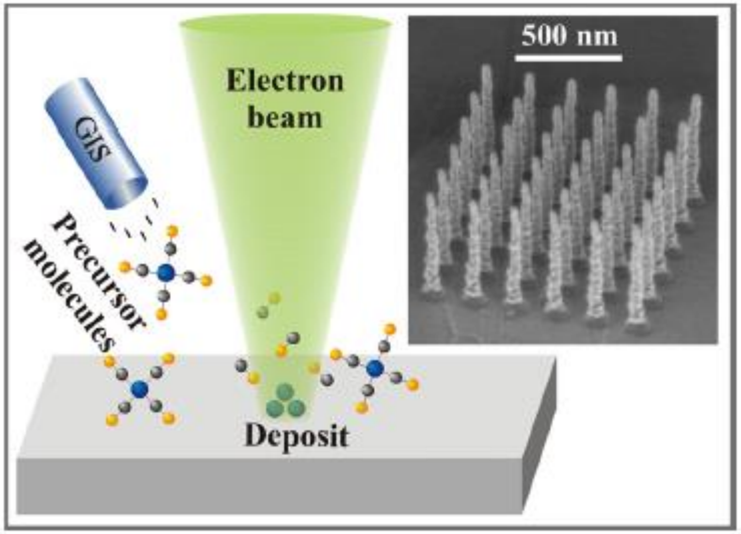

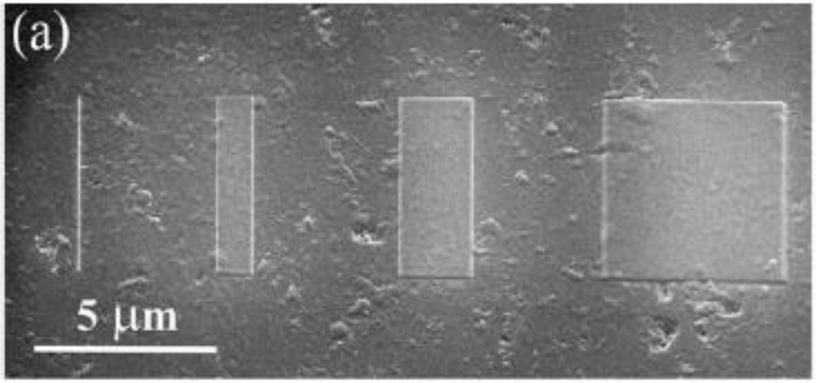

Scanning electron microscopy image of the set of EBID cobalt structures

Magnetometry of ultra-small nanostructure

Single sweep

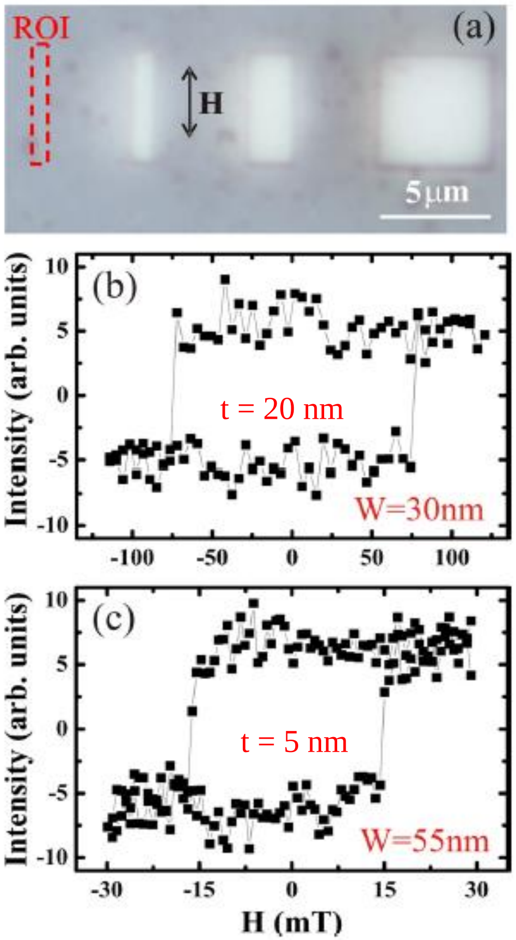

9 averages

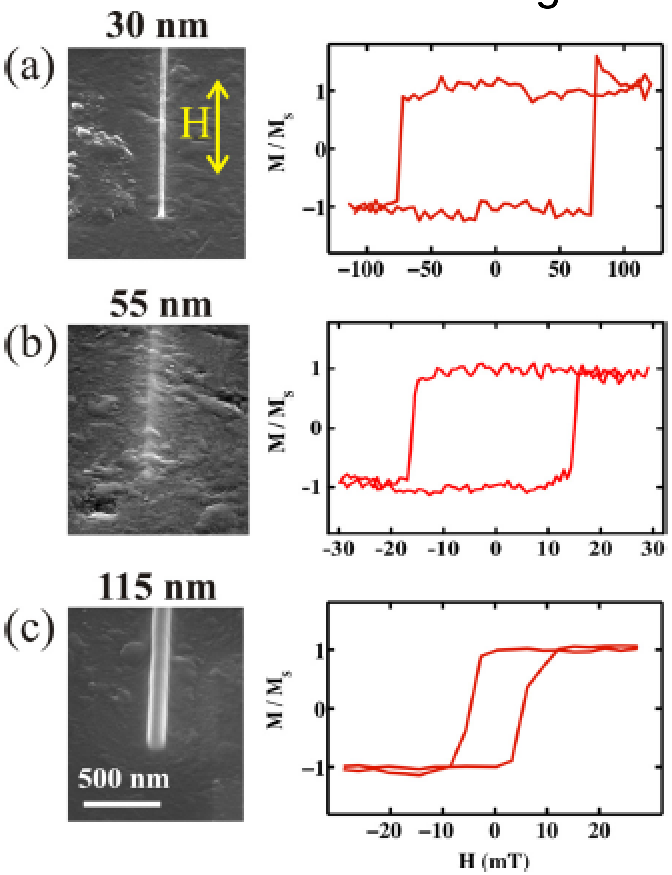

single sweep measurement sensitivity of approximately 1 x10^{-15} Am^2
sensitivity of 10^{-12} to 10^{-13} Am^2 for the latest generation of SQUID magnetometer

APPLIED PHYSICS LETTERS 100, 142401 (2012)

Diffraction of light by an array

As is well known for optical gratings, when a beam of light is incident upon a sample that has a structure comparable to the wavelength of radiation, the beam is not only reflected but is also diffracted. If the material is magnetic, one may ask whether the diffracted beams also carry information about the magnetic structure.

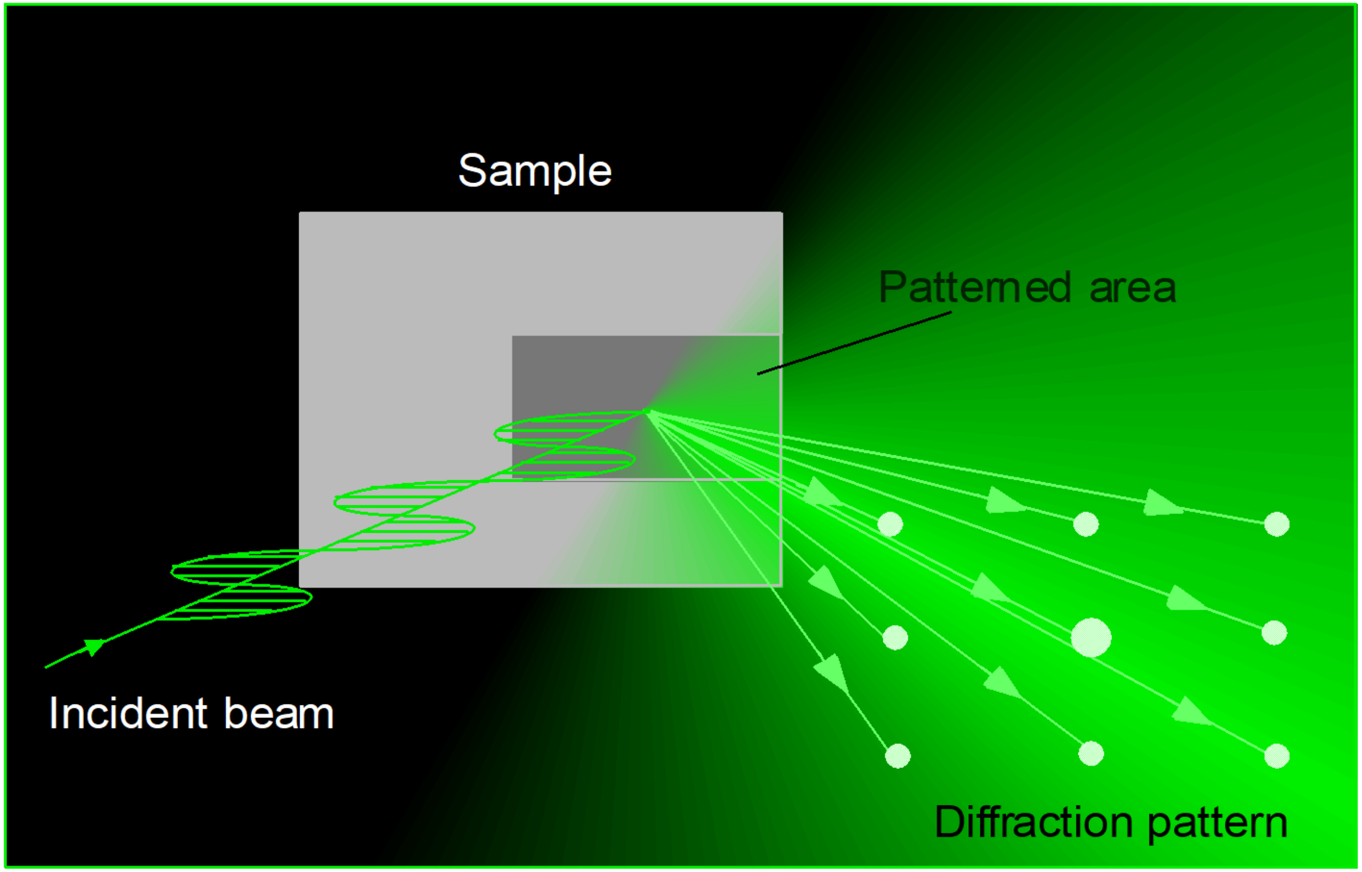

"Diffracted-MOKE: What does it tell you?",
M. Grimsditch and P. Vavassori J. Phys.: Condensed Matter **16**, R275 - R294 (2004).

Examples of D-MOKE loops

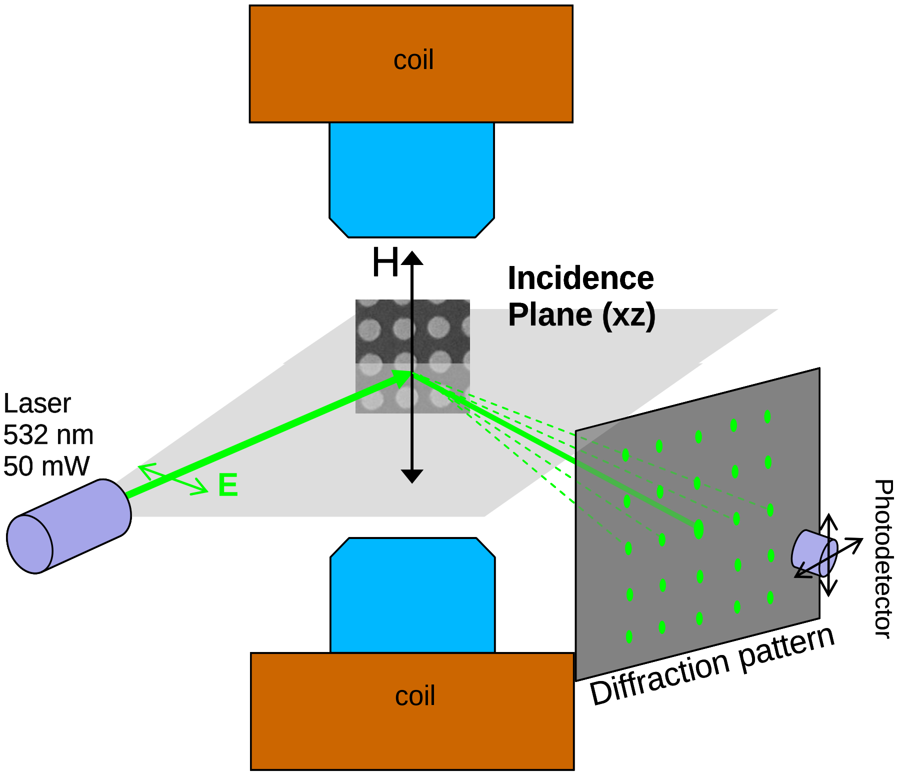

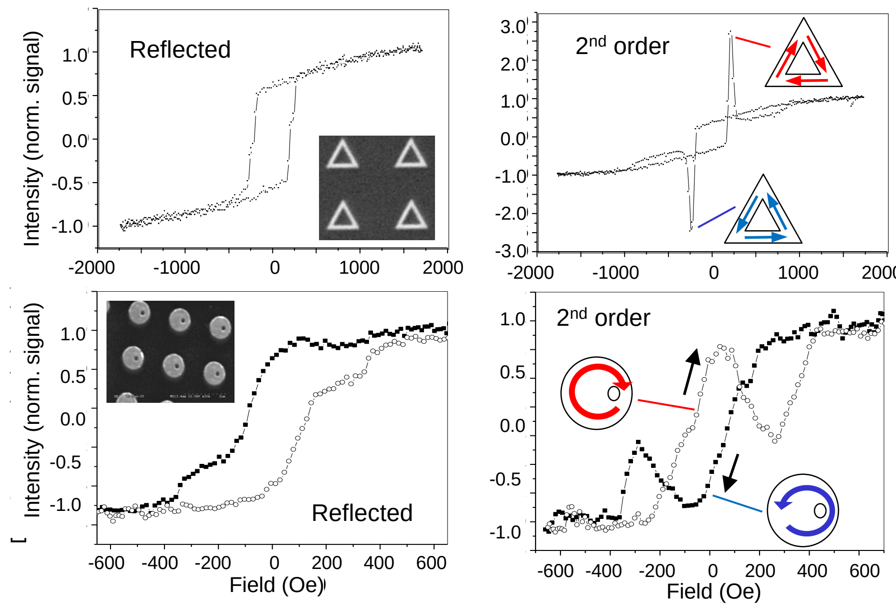

Peculiar structures due to
- Collective properties
- Interference effects

P. Vavassori, et al.,Phys. Rev. B **59** 6337 (1999)
M. Grimsditch, P. Vavassori, et al., Phys. Rev. B **65**, 172419 (2002)
P. Vavassori, et al., Phys. Rev. B **67**, 134429 (2003)
P. Vavassori, et al., Phys. Rev. B **69**, 214404 (2004)
P. Vavassori, et al., J Appl. Phys. **99**, 053902 (2006)
P. Vavassori, et al., J. Appl. Phys. **101**, 023902 (2007)
P. Vavassori, et al., Phys. Rev. B **78**, 174403 (2008)

Intuitive explanation of D-MOKE loops

$$r_{pp} = r^o_{pp} + r^m_{pp} m_y(x,y)$$

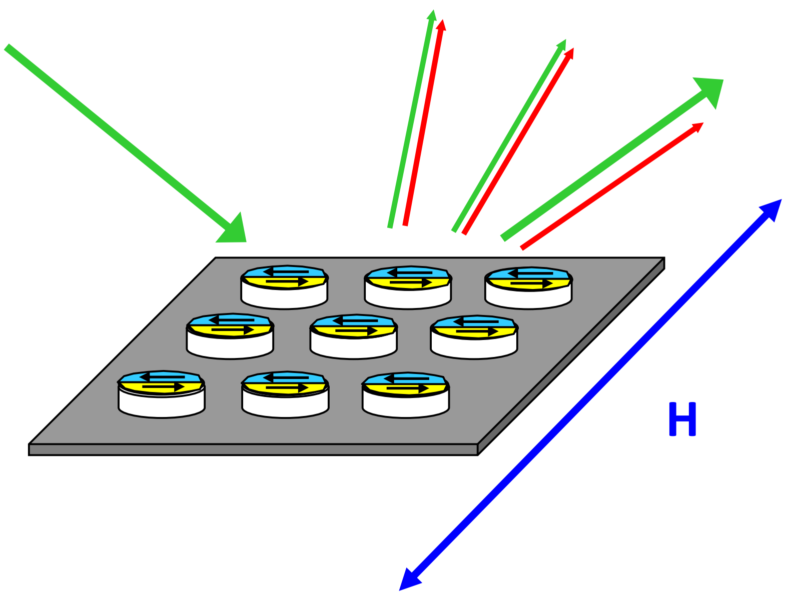

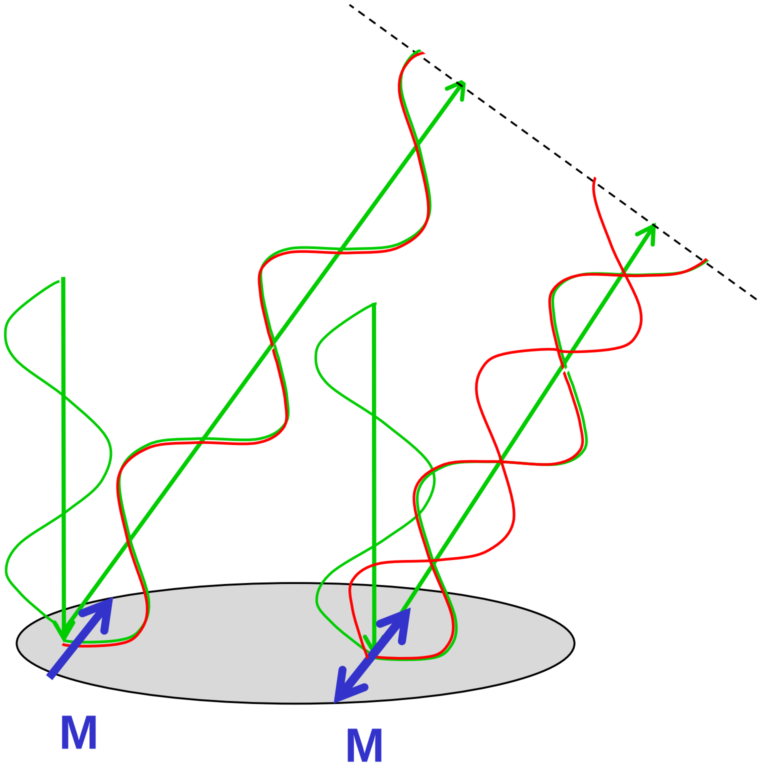

Peculiar structures due to
- Interference effects
- Collective properties

O. Geoffroy et al., J. Magn. Magn. Mat. **121** (1993) 516
Y. Souche et al., J. Magn. Magn. Mat., **140-144** (1995) 2179

Simple theory of diffracted-MOKE

Physical-optics approximation provides a very simple and physically transparent description.

The electric field in the nth order diffracted beam, due to the periodic modulation of the “effective” reflectivity $\mathbf{r'_{pp}}$ is:

$$\mathbf{E^n_d} = \mathbf{E_o} f_n$$

$$f_n = \int_S r'_{pp} \exp\{i\, n\, \mathbf{G}\cdot\mathbf{r}\}\, dS$$

where **n** integer, **G** reciprocal lattice vector and **S** is the unit cell.

$$r'_{pp} = r^o_{pp} + r^m_{pp}\, m_y(x,y,H)$$

$$\mathbf{E_n^d} = \mathbf{E_o}\,(r^o_{pp} f_n^{nm} + r^m_{pp} f_n^{m})$$ with $r^o_{pp}(\theta_i, \theta_n, \varepsilon_{dots}, \varepsilon_{subst})$, $r^m_{pp}(\theta_i, \theta_n, \varepsilon_{dots}, Q)$

$$f_n^{nm} = \int_S \exp\{i\, n\, \mathbf{G}\cdot\mathbf{r}\}\, dxdy$$ ← **non-magnetic form factor**

$$f_n^{m}(H) = \int_{Dot} m_y(x,y,H) \exp\{i\, n\, \mathbf{G}\cdot\mathbf{r}\}\, dxdy$$ ← **magnetic form factor**

$$I_n^d = \mathbf{E_n^d}\,(\mathbf{E_n^d})^*$$

$$\Delta \mathbf{I_n^m}\,(\mathbf{m_y}) = A_n \mathrm{Re}[f_n^m] + B_n \mathrm{Im}[f_n^m]$$

What are the differences due to?

Diffracted spots in the scattering plane

$G_x = 2\pi/L$ reciprocal lattice vector

$\Delta I_n^m \propto A_n \, Re[f_n^m] + B_n \, Im[f_n^m]$

$Re[f_n^m] = \int_{Dot} m_y \cos(n \, G_x \, x) \, dS$

$Im[f_n^m] = \int_{Dot} m_y \sin(n \, G_x \, x) \, dS$

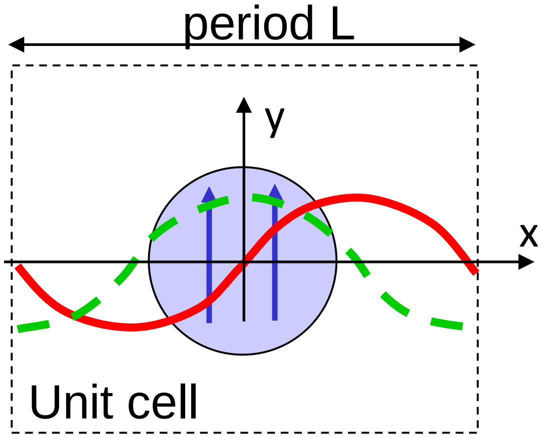

Saturated state ⇒ $Im[f_1^m] = 0$, $Re[f_1^m] > 0$

Two-domain state: asymmetric M distribution

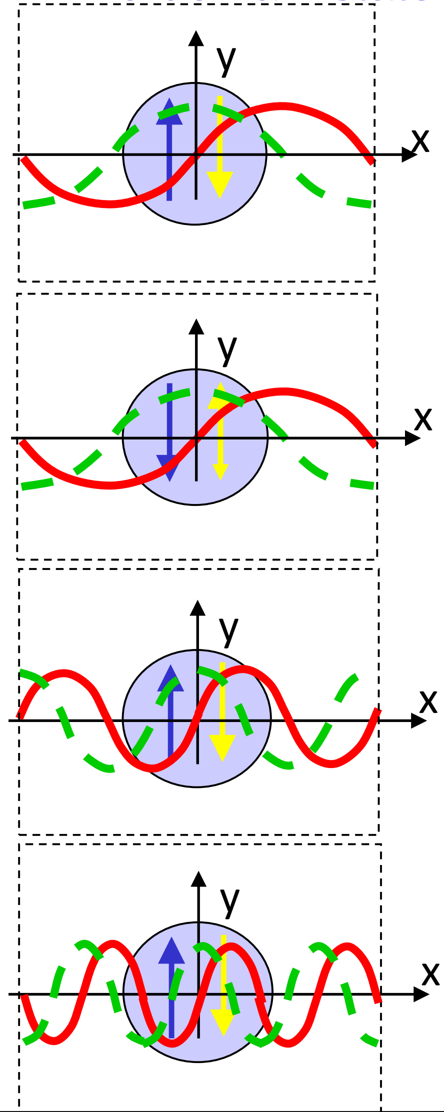

1st order

⇒ $Im[f_1^m] < 0$, $Re[f_1^m] = 0$

⇒ $Im[f_1^m] > 0$, $Re[f_1^m] = 0$

2nd order

⇒ $Im[f_2^m] < 0$ **large**, $Re[f_2^m] = 0$

3rd order

⇒ $Im[f_2^m] < 0$ **very large**, $Re[f_2^m] = 0$

Tuning the sensitivity to selected portions of the dot!

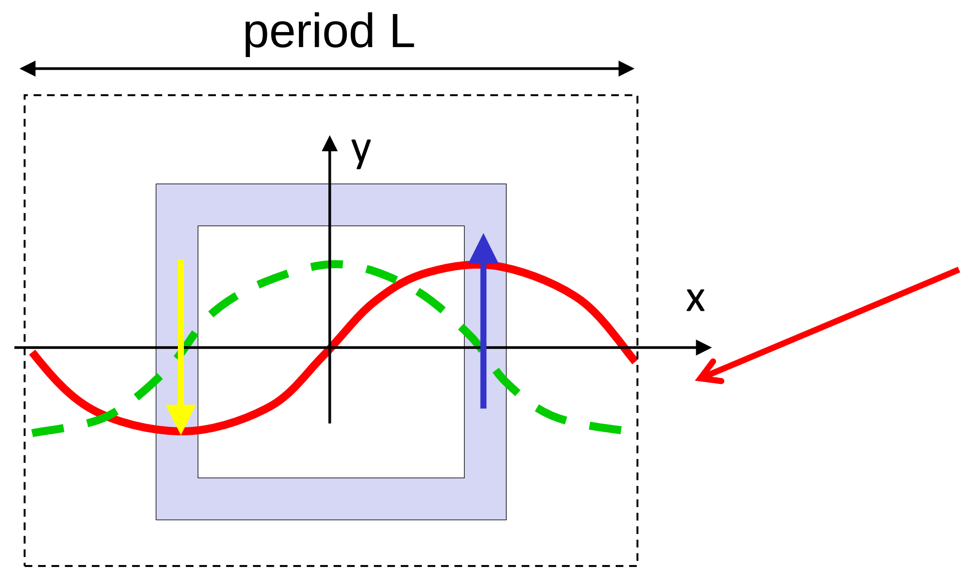

Immaginary contribution:
highlight any asymmetric
(y-mirror symmetry breaking)
magnetic (m_y) behaviour

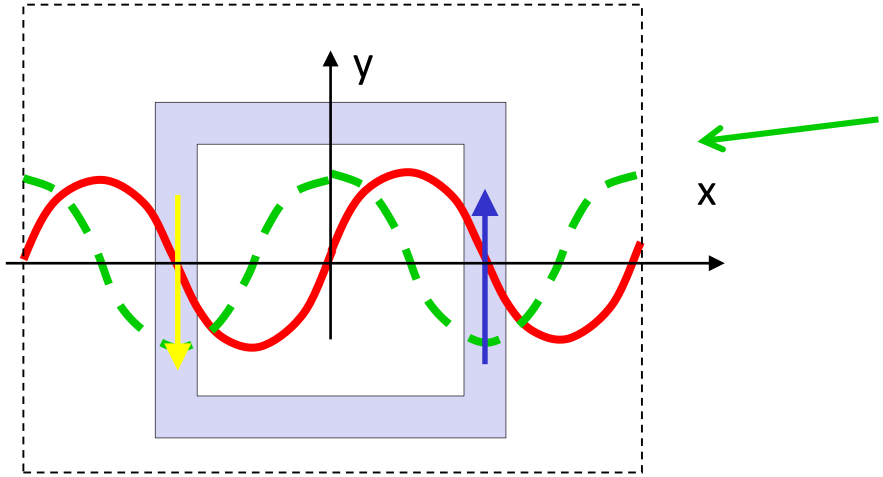

Real contribution:
y-mirror symmetry m_y

Asymmetry to induce the desired vortex rotation

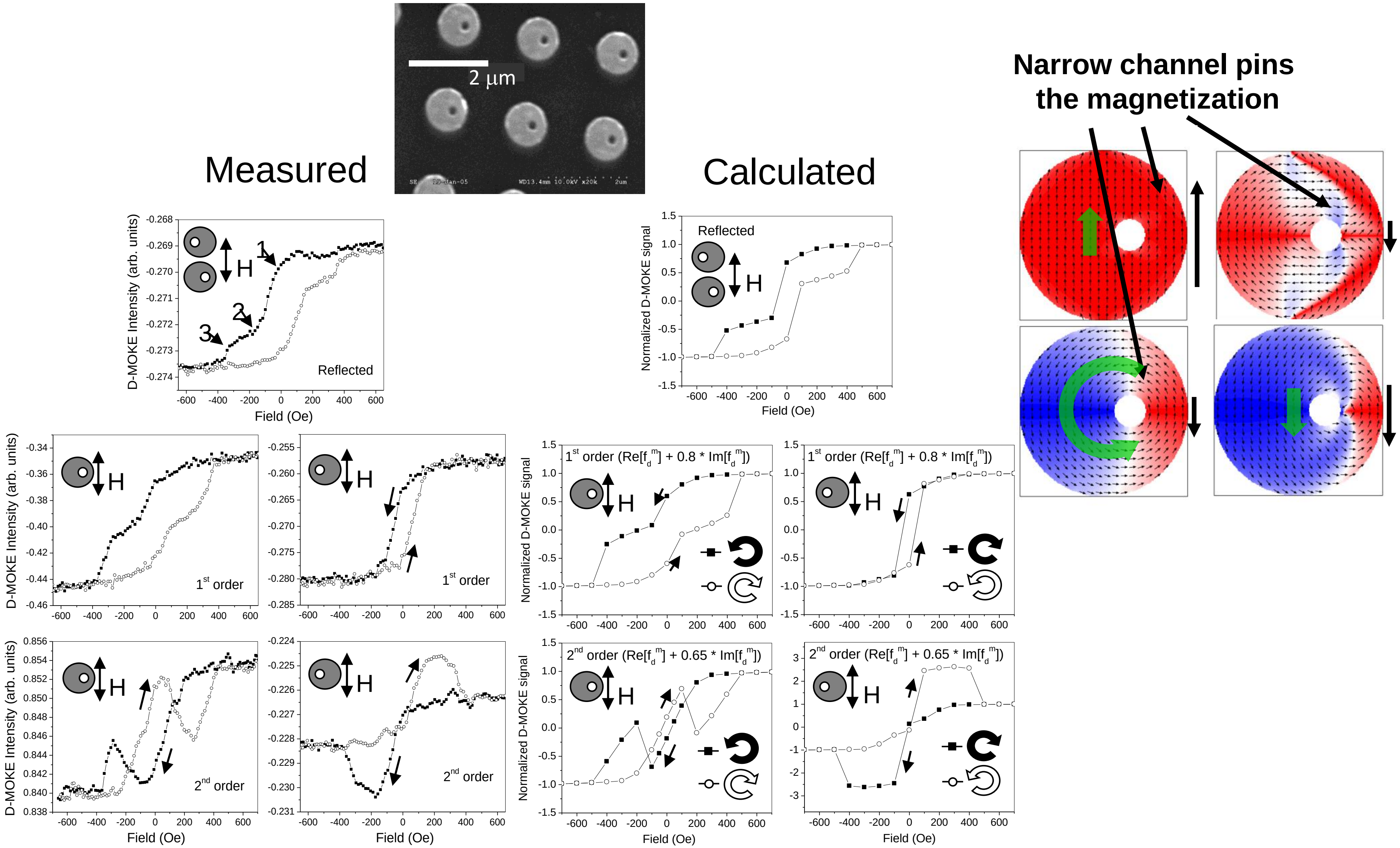

P. Vavassori, R. Bovolenta, V. Metlushko, and B. Ilic, J Appl. Phys. **99**, 053902 (2006)

Measured D-MOKE loops from square rings

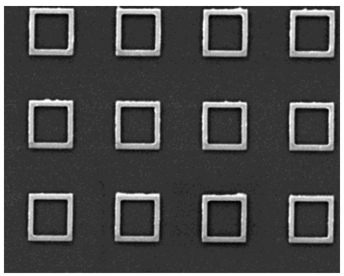

Square lattice (4.1x4.1 μm^2) of Permalloy square rings (2.1 μm side). Nominal width 250 nm. Thickness 30 nm.

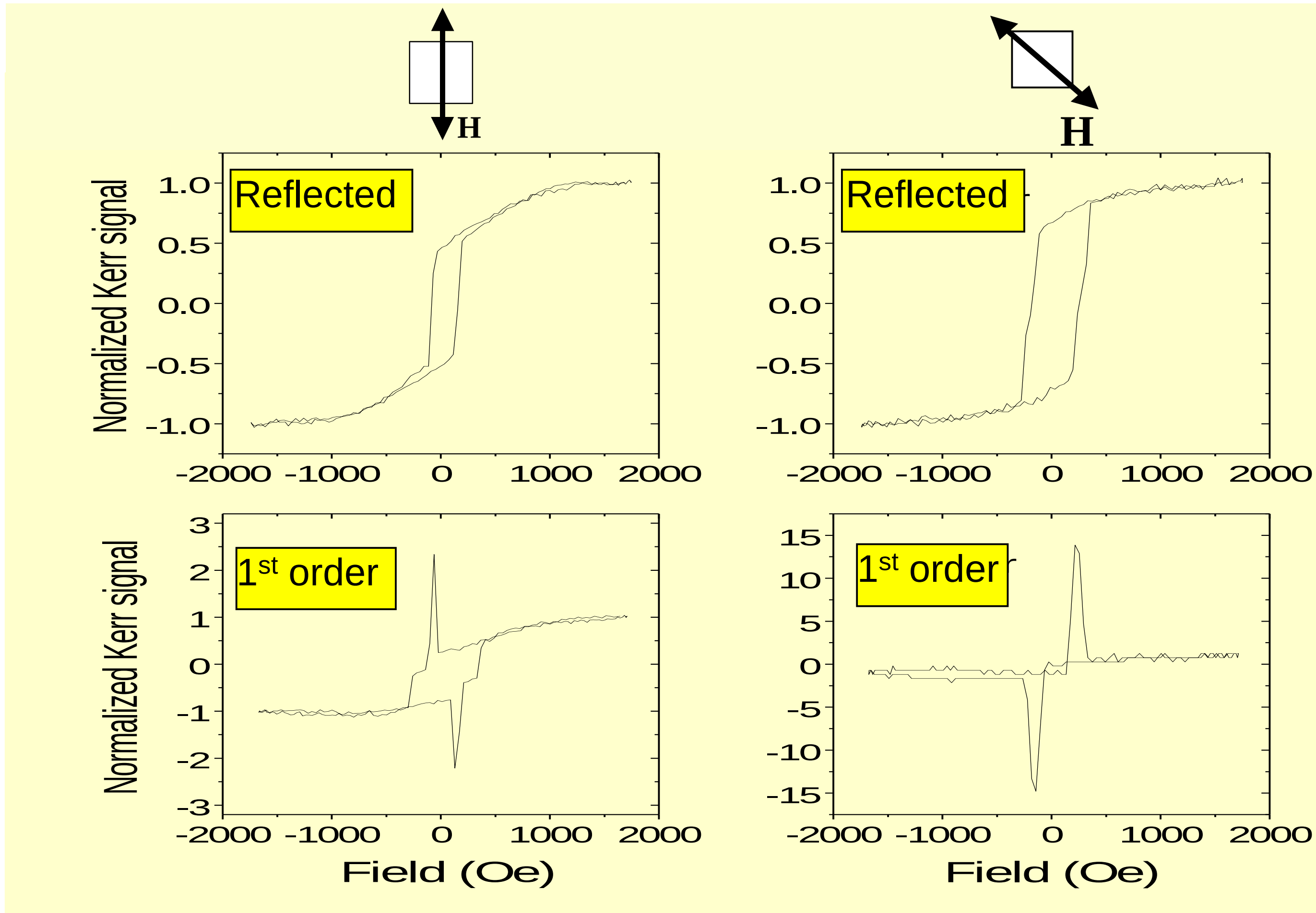

P. Vavassori, et al., Phys. Rev. B **67**, 134429 (2003)

Note intense peaks in the diffracted loops

Square ring structures

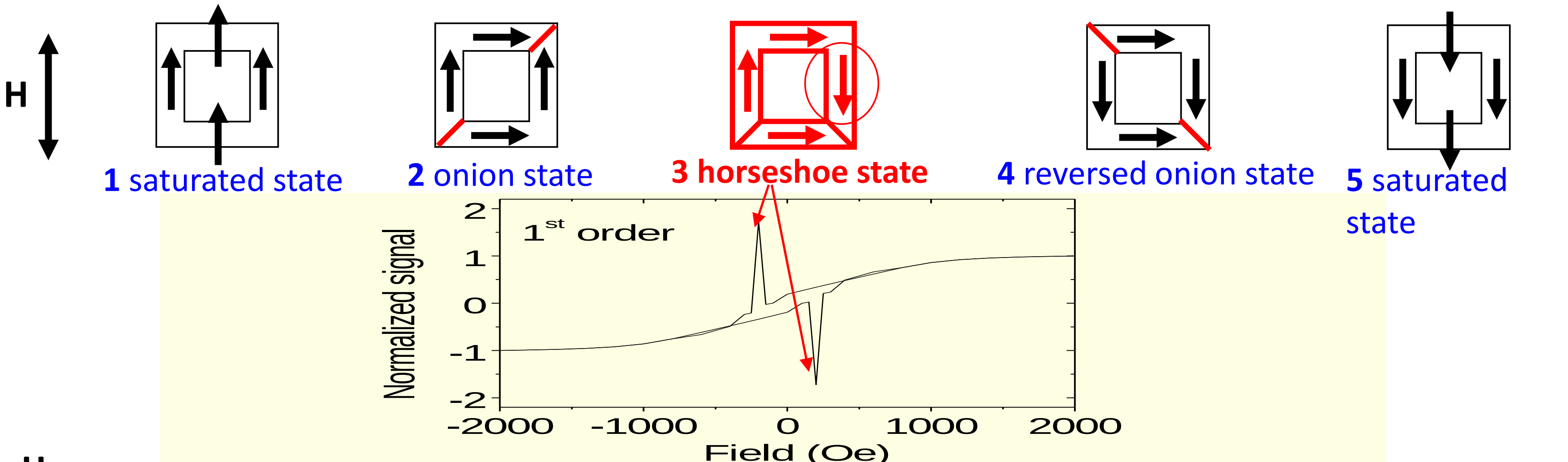

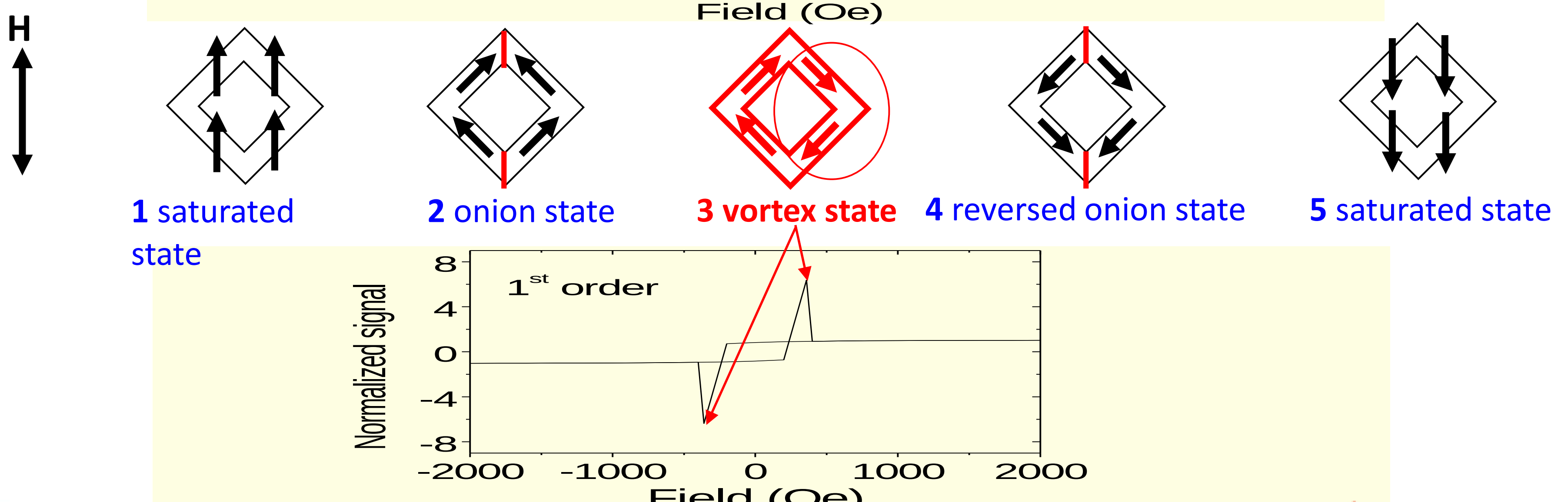

Quenching structures in intermediate states and image them with MFM

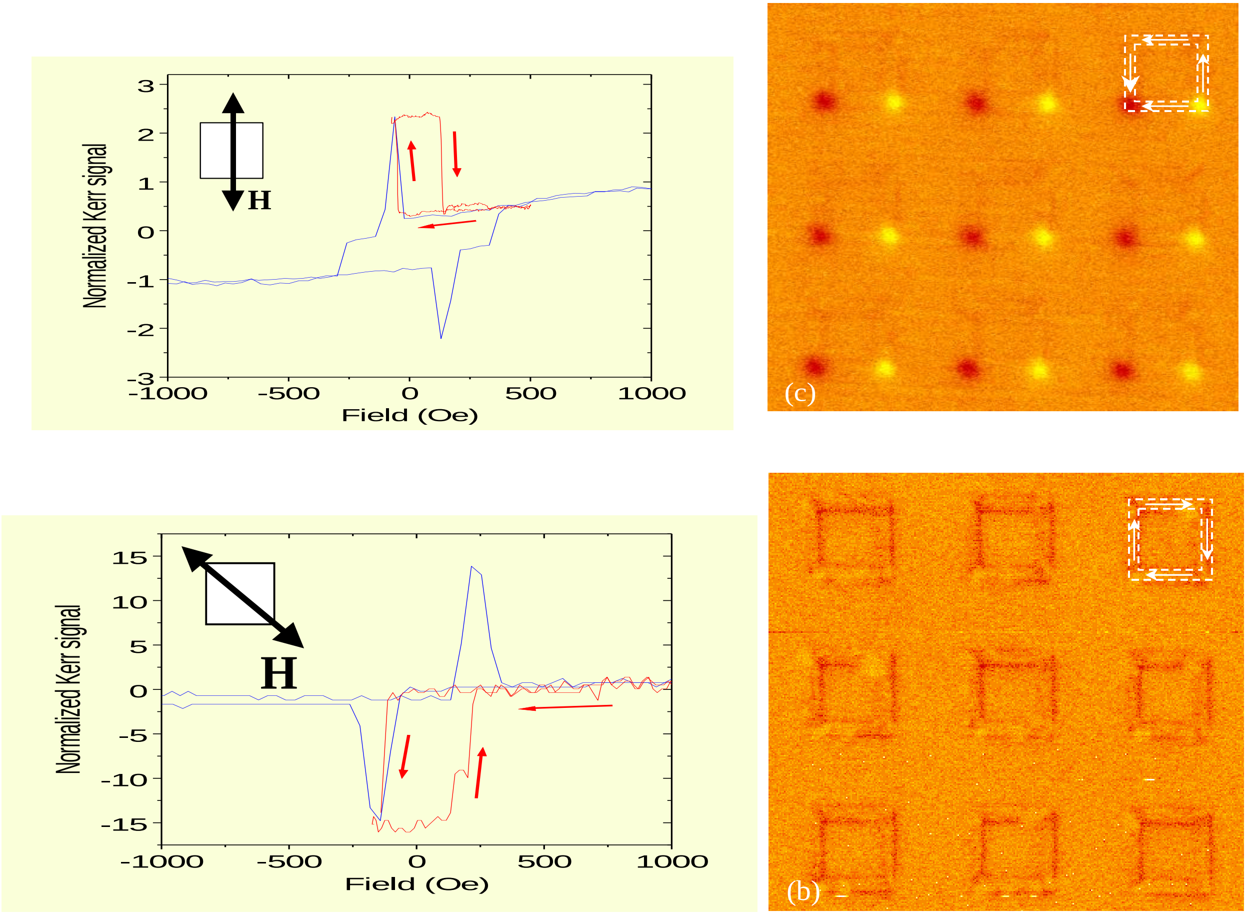

P. Vavassori, M. Grimsditch, V. Novosad, V. Metlushko, B. Ilic, P. Neuzil, and R. Kumar, Phys. Rev. B **67**, 134429 (2003)

About A_n and B_n

$\Delta I_n^m (m_y) = 2 f_n^{nm} \{ A_n \mathrm{Re}[f_n^m] + B_n \mathrm{Im}[f_n^m] \}$

A_n and B_n $(\theta_i, \theta_n, \varepsilon_{dots}, \varepsilon_{sub}, Q)$

$A_n = \mathrm{Re}[r^o_{pp}{}^* \, r^m_{pp}]$

$B_n = \mathrm{Im}[r^o_{pp}{}^* \, r^m_{pp}]$

$r'_{pp} = r^o_{pp} + r^m_{pp}$ “effective” reflectivity

Y. Suzuki, C. Chappert, P. Bruno, and P. Veillet, *J. Magn. Magn. Mater.* ***165*** 516 (1997) only for size >> λ

For inhomogeneous gratings $r^o_{pp} = r^o_{pp,\,dot} + r^o_{pp,\,sub}$

An interesting characteristic of D-MOKE related to this : the absolute value of $(\Delta I/I_o)_n$ is increased up to several times the specular value. Effect due to the compensation of the non-magnetic component of the light diffracted by the magnetic dots and the light diffracted by the (non-magnetic) complementary part of the substrate.

$I_{o,n} = |r^o_{pp,\,dot}|^2 f_n^{nm} + |r^o_{pp,\,sub}|^2 f'^{nm}_n = (|r^o_{pp,\,dot}|^2 - |r^o_{pp,\,sub}|^2) f_n^{nm}$

Different approach: towards Fourier imaging? 1st step

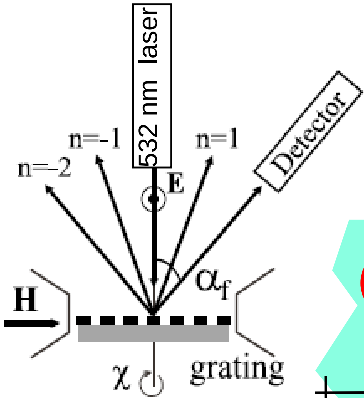

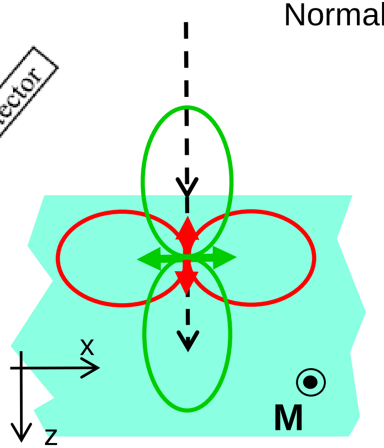

Normal incidence: the scattering plane is defined by the selected spot

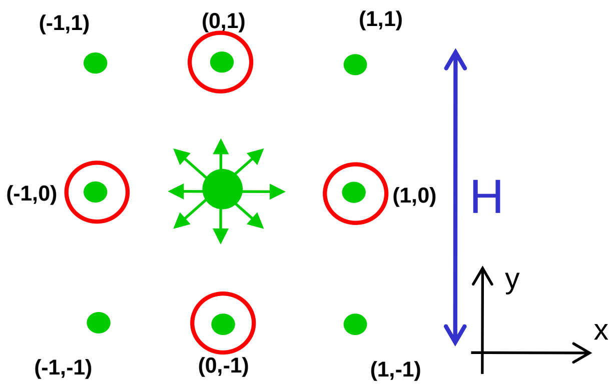

Sensitivity to (m_x , m_y)

Sensitivity to m_y

$$(\Delta I_n^m)_{norm} = A_n \,\mathrm{Re}[f_n^m] - B_n \,\mathrm{Im}[f_n^m]$$

$$(\Delta I_{-n}^m)_{norm} = -A_n \,\mathrm{Re}[f_n^m] - B_n \,\mathrm{Im}[f_n^m]$$

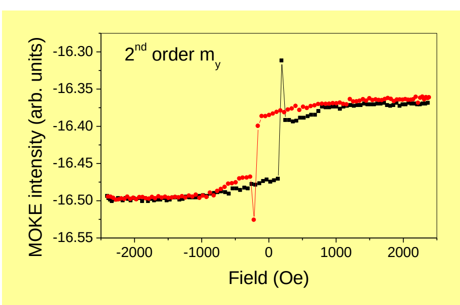

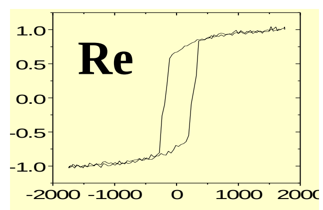

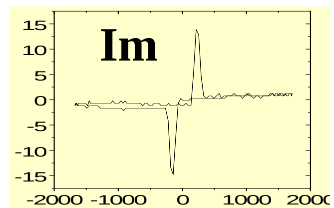

Sensitivity to m_x

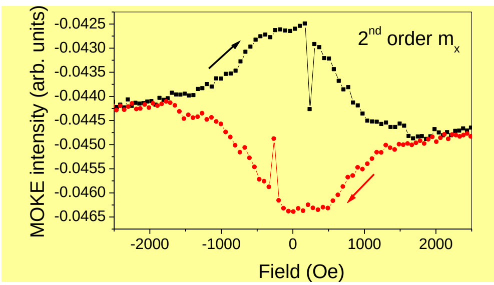

Vectorial D-MOKE

D-MOKE problem fully solved

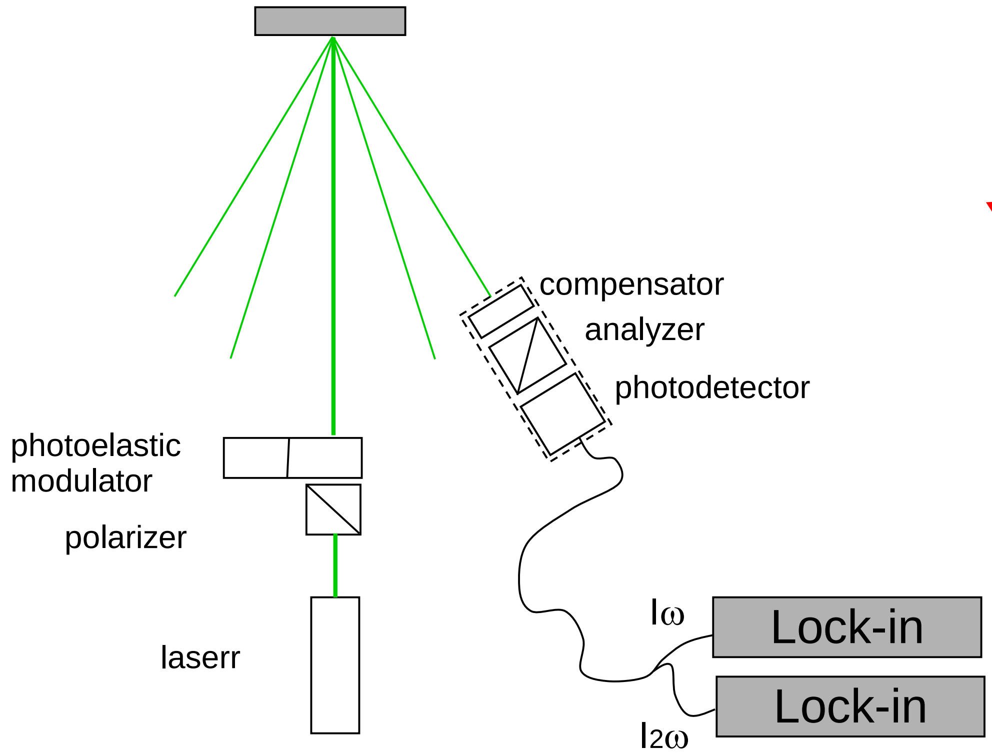

$\mathrm{Im}[\Delta r_m/r_0] = \Delta\phi_m/\phi_0$

$\mathrm{Re}[\Delta r_m/r_0] = \Delta I_m/I_0$

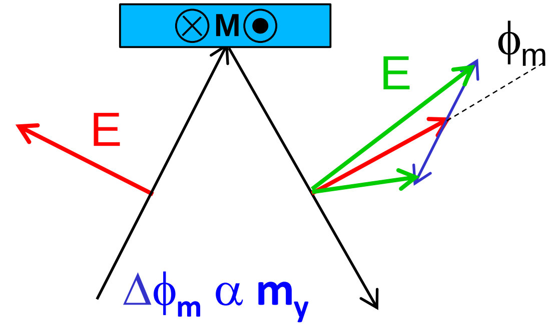

$\Delta I^n{}_m/I^n{}_o = A_n\,\mathrm{Re}[f_n{}^m] - B_n\,\mathrm{Im}[f_n{}^m]$

$\Delta\phi^n{}_m/\phi^n{}_o = B_n\,\mathrm{Re}[f_n{}^m] - A_n\,\mathrm{Im}[f_n{}^m]$

$\Delta I^{-n}{}_m/I^{-n}{}_o = -A_n\,\mathrm{Re}[f_n{}^m] - B_n\,\mathrm{Im}[f_n{}^m]$

$\Delta\phi^{-n}{}_m/\phi^{-n}{}_o = -B_n\,\mathrm{Re}[f_n{}^m] - A_n\,\mathrm{Im}[f_n{}^m]$

⇒ $\mathrm{Re}[f_n{}^m]$, $\mathrm{Im}[f_n{}^m]$

K. Postava et al. “Null ellipsometer with phase modulation,” Opt. Express **12**, 6040 (2004)

Samples: arrays of NiFe triangular rings

Electron beam lithography

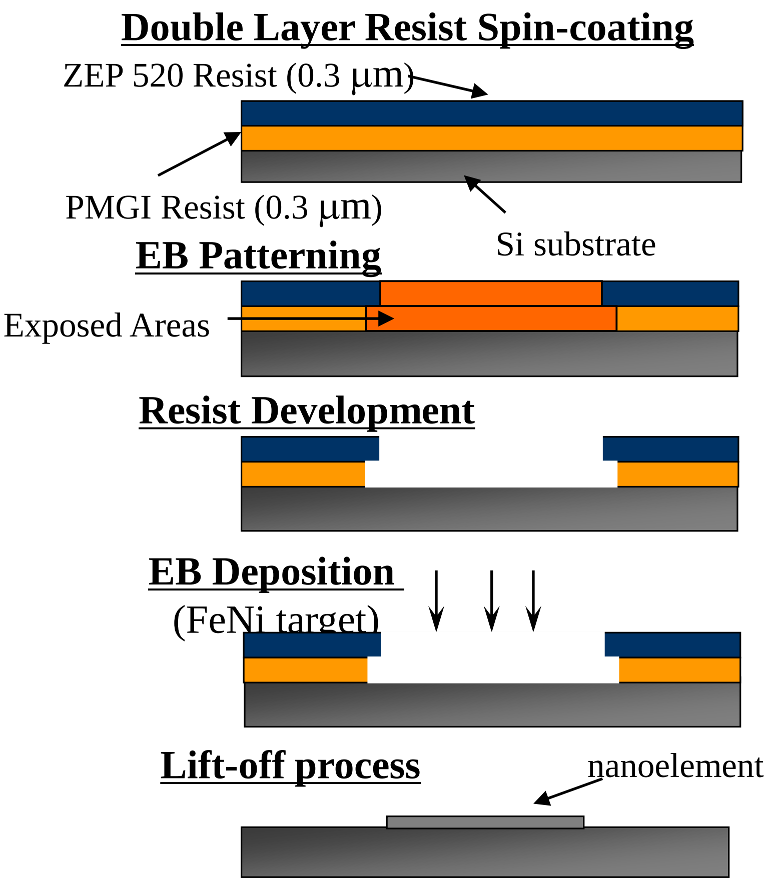

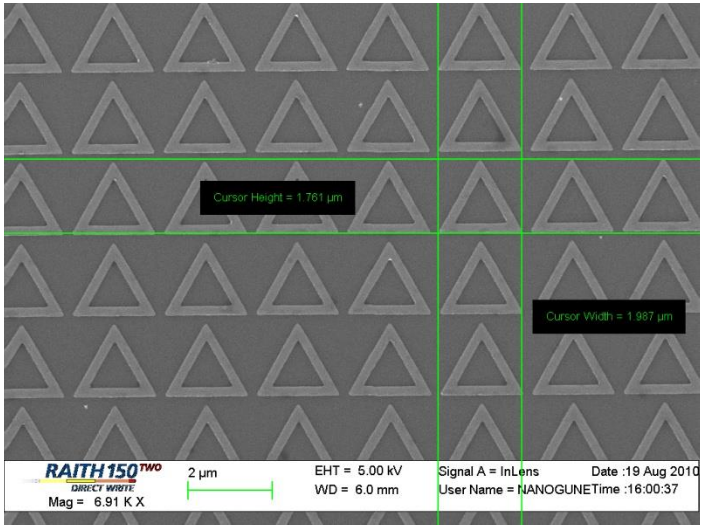

Triangular rings (2.1 µm side).
Nominal width 250 nm.
Nominal thickness 30 nm.

Normal incidence: extraction of magnetic form factors

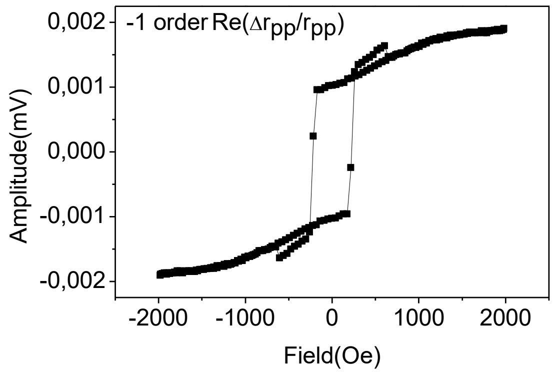

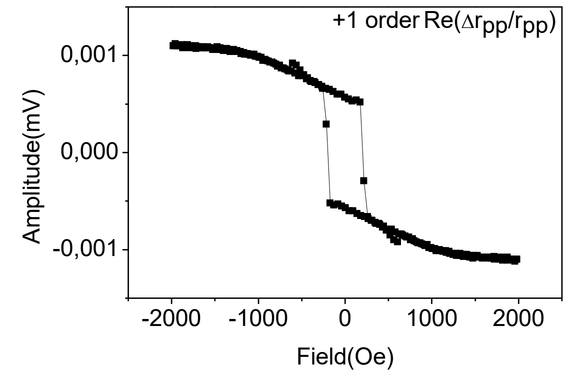

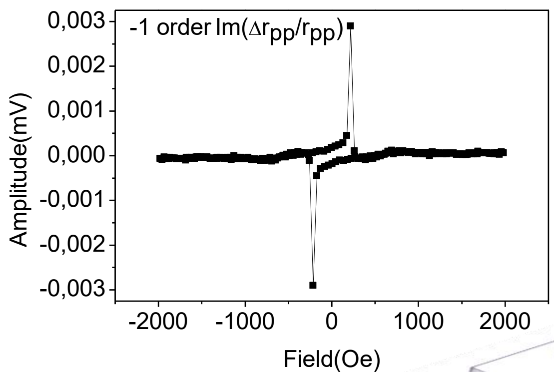

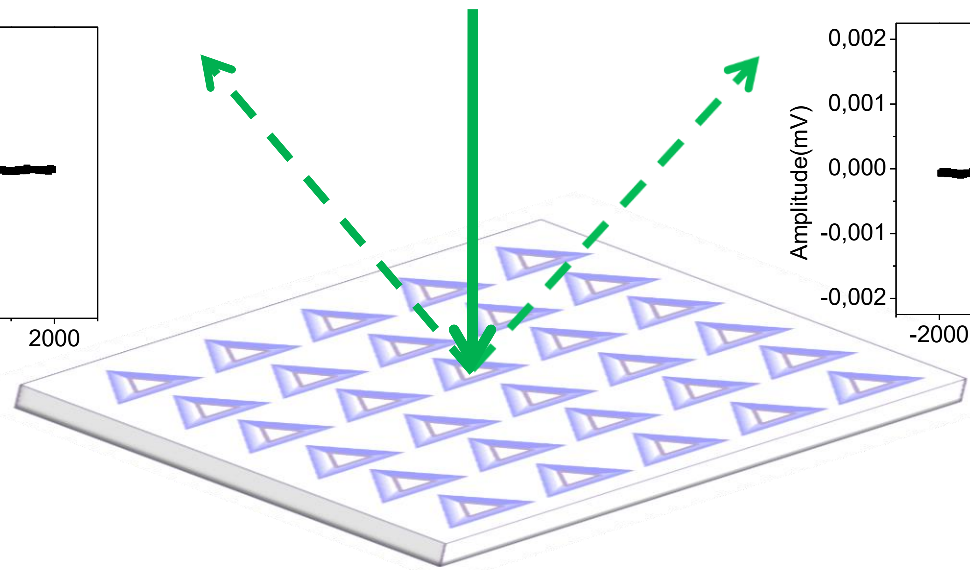

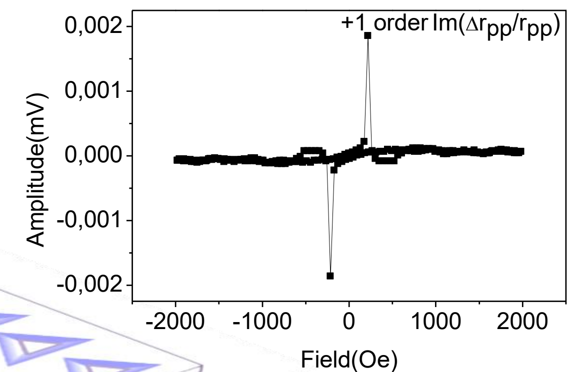

$\Delta I^{n}{}_{m}/I^{n}{}_{o} = A_n\,\mathrm{Re}[f_n{}^{m}] - B_n\,\mathrm{Im}[f_n{}^{m}]$

$\Delta I^{-n}{}_{m}/I^{-n}{}_{o} = -A_n\,\mathrm{Re}[f_n{}^{m}] - B_n\,\mathrm{Im}[f_n{}^{m}]$

$\Delta \phi^{n}{}_{m}/\phi^{n}{}_{o} = B_n\,\mathrm{Re}[f_n{}^{m}] - A_n\,\mathrm{Im}[f_n{}^{m}]$

$\Delta \phi^{-n}{}_{m}/\phi^{-n}{}_{o} = -B_n\,\mathrm{Re}[f_n{}^{m}] - A_n\,\mathrm{Im}[f_n{}^{m}]$

⇒ $\mathrm{Re}[f_n{}^{m}]$, $\mathrm{Im}[f_n{}^{m}]$

Exp and calculated Re[f_m] and Im[f_m] – horizontal and vertical plane

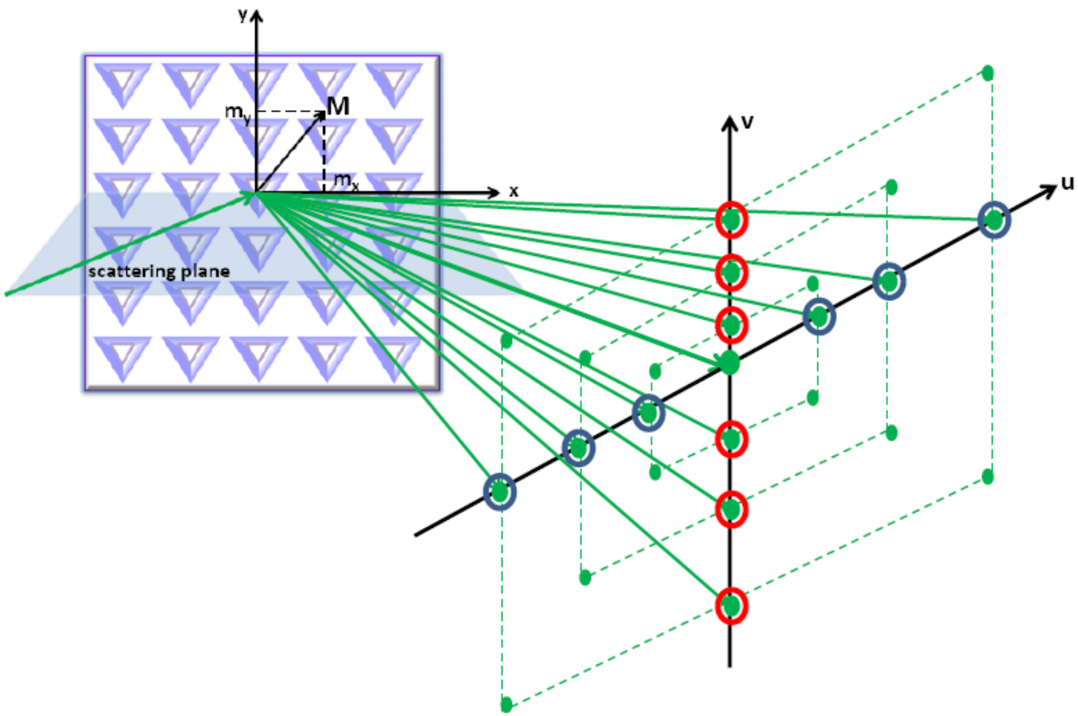

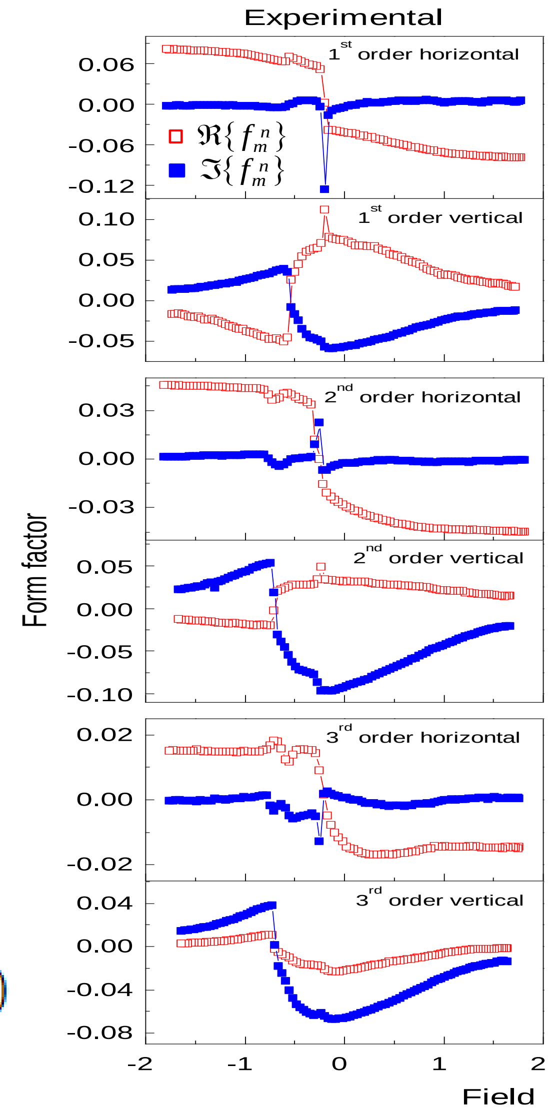

$$m_\perp(\vec{r}) = \sum_{n=-3}^{3} f_n^m e^{-i(n\vec{G}\cdot\vec{r})} = \sum_{n=-3}^{3} Im[f_n^m]\sin(n\vec{G}\cdot\vec{r}) + Re[f_n^m]\cos(n\vec{G}\cdot\vec{r})$$

Re and Im parts of the magnetic form factors

1^{st} - h

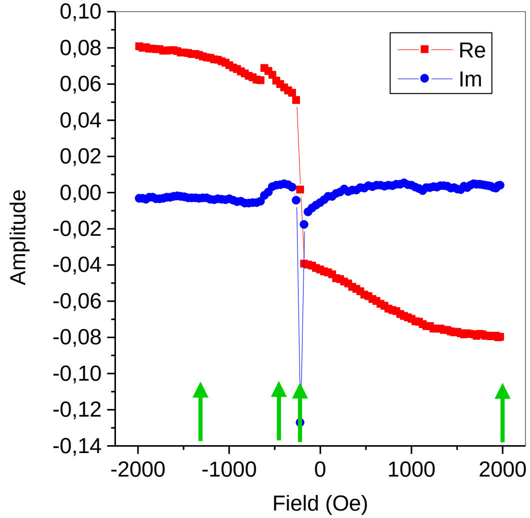

2^{nd} - h

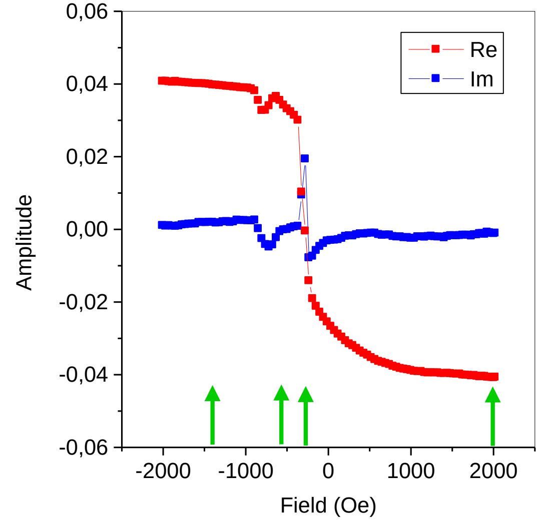

3^{rd} - h

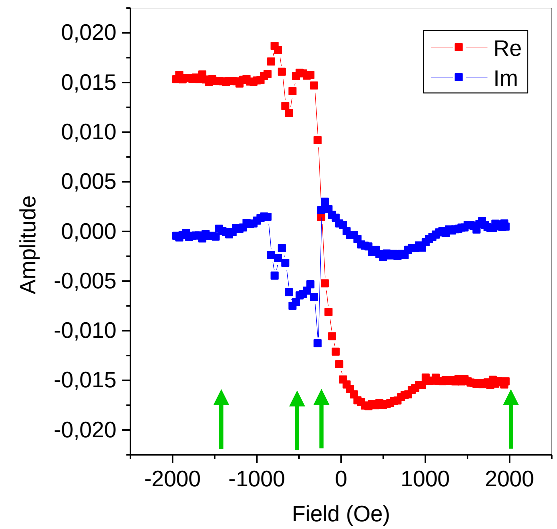

1^{st} - v

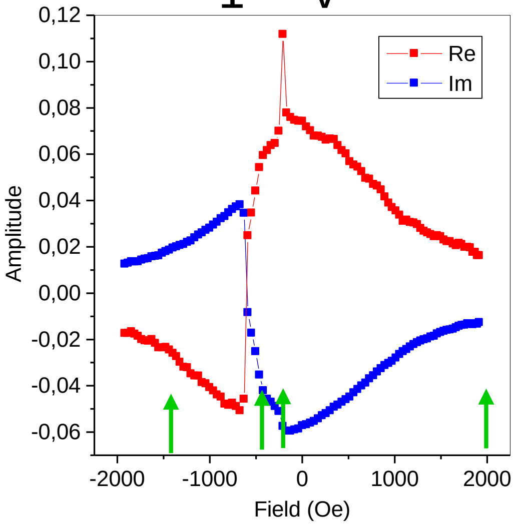

2^{nd} - v

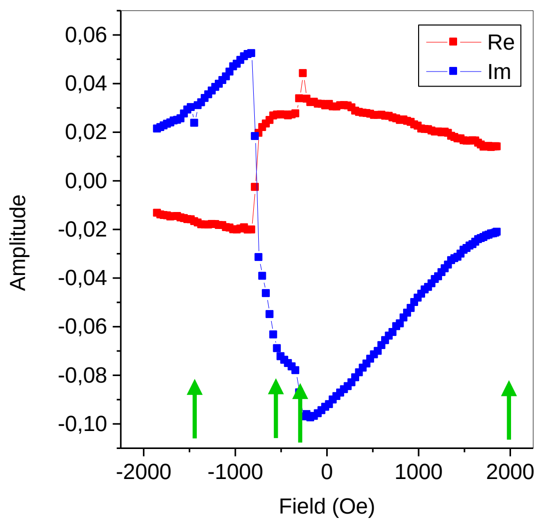

3^{rd} - v

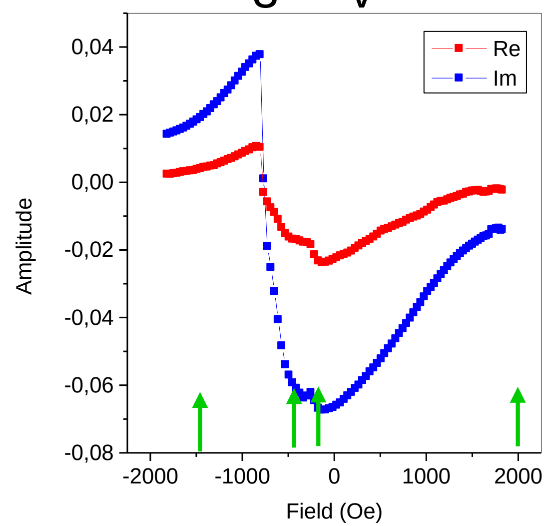

Saturated state

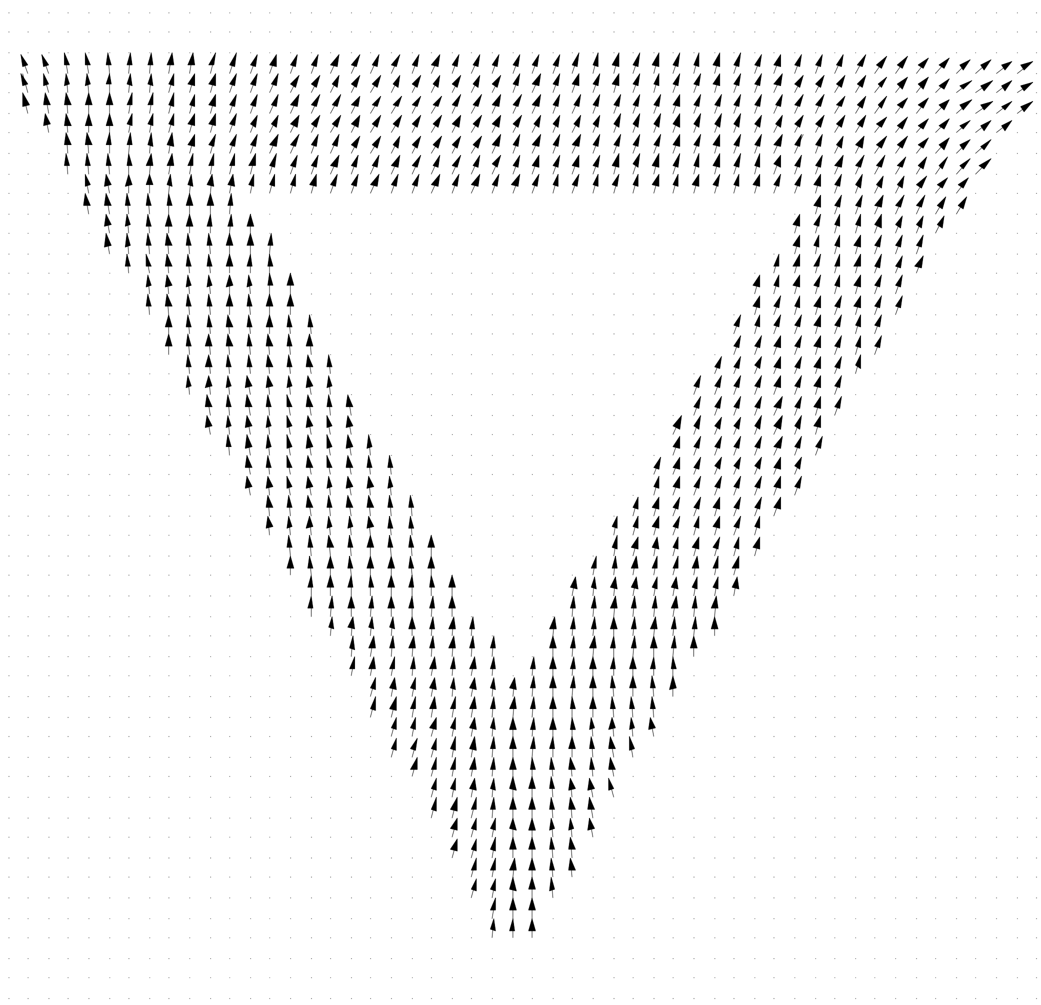

"Peak" state

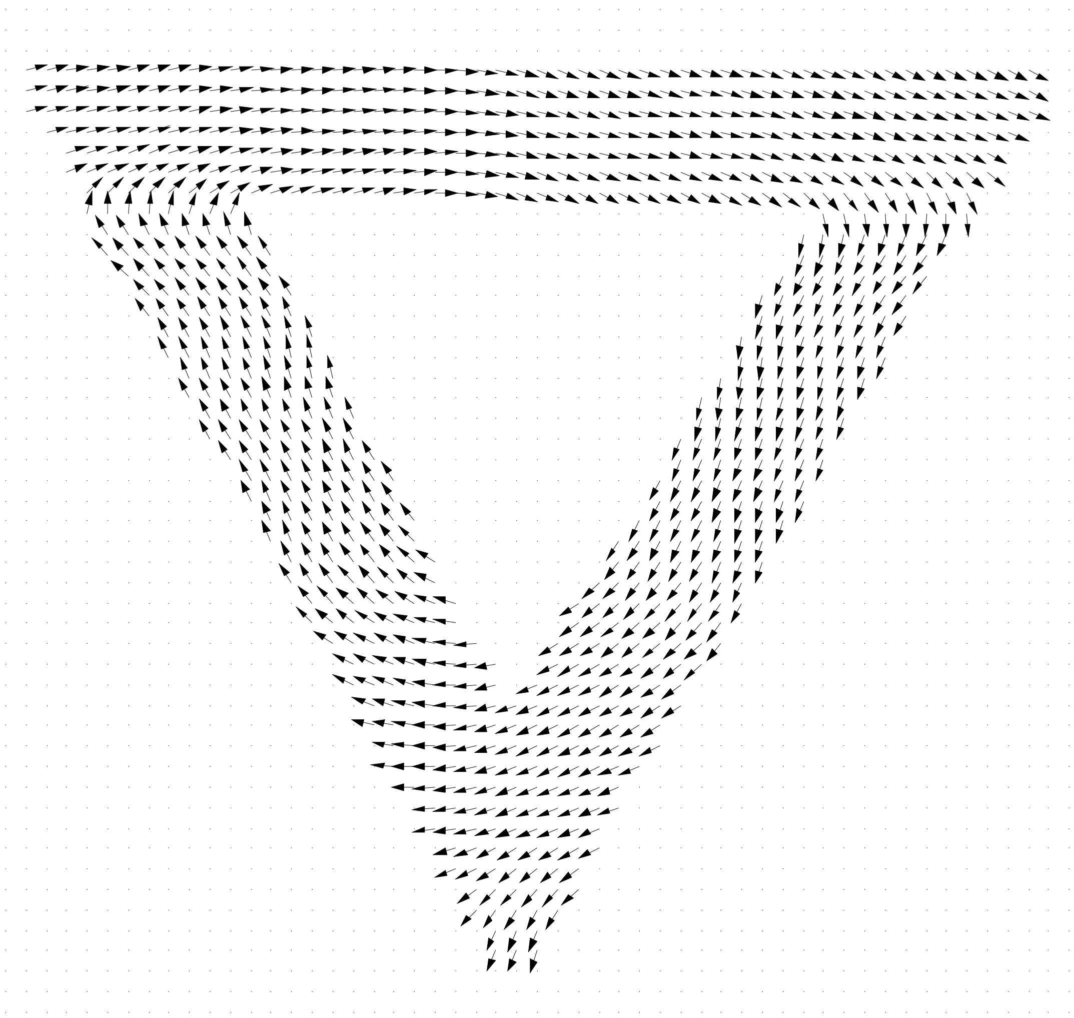

After "peak"

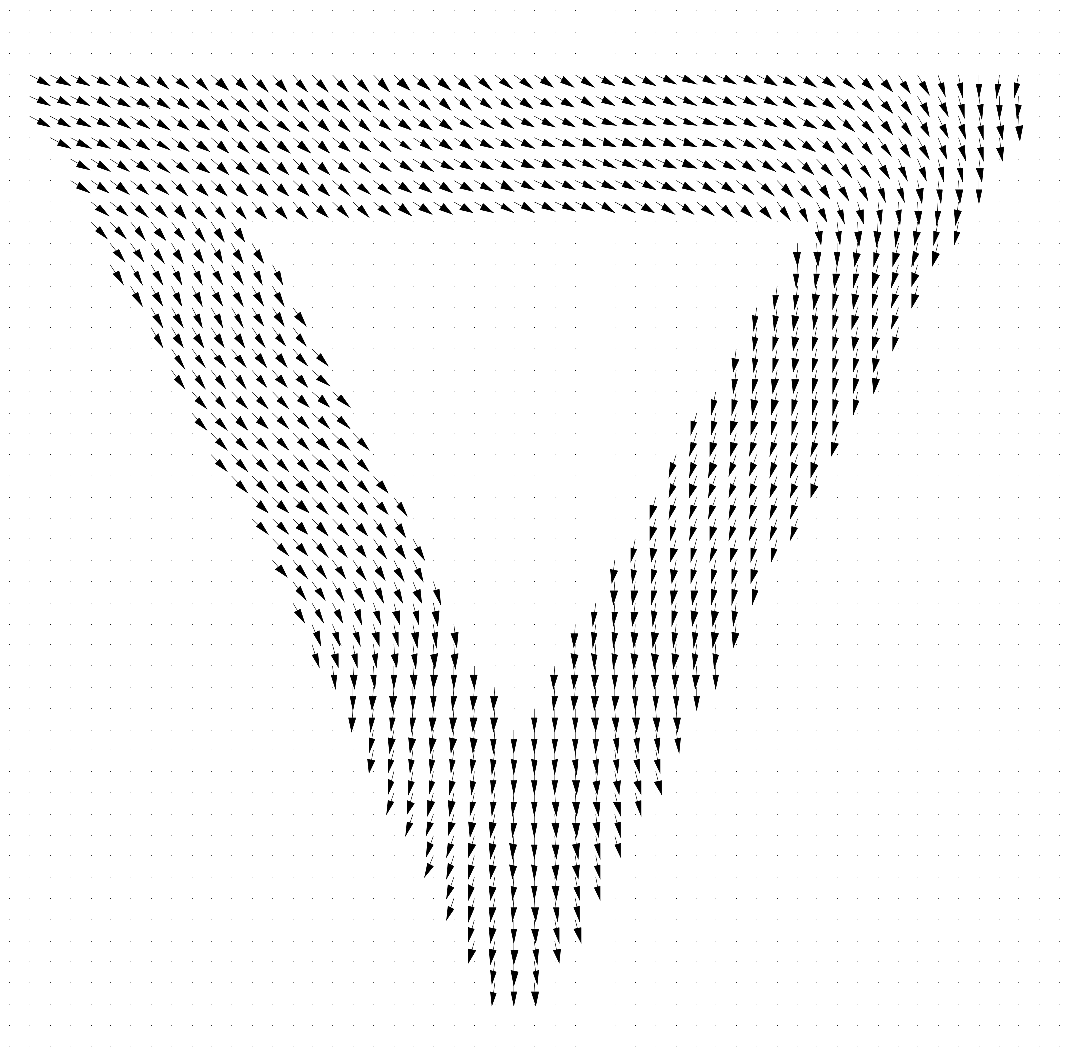

Towards negative saturation

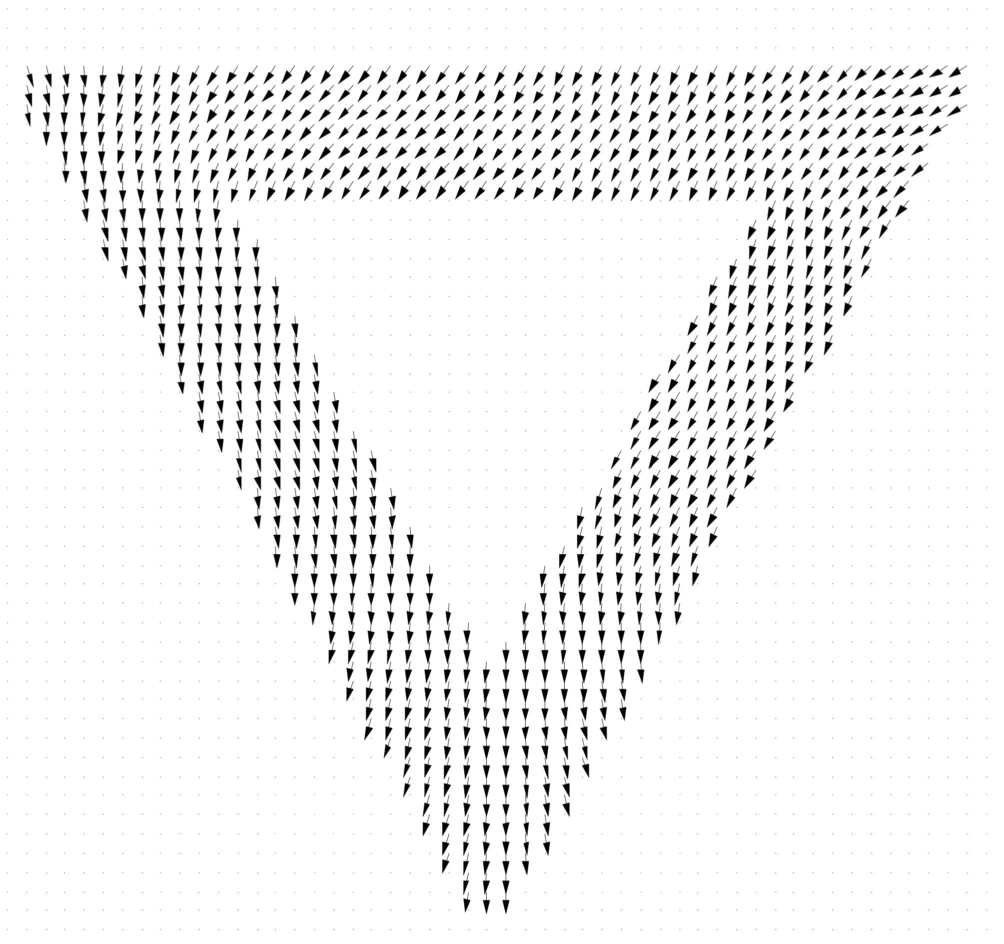

Exp and calculated Re[f_m] and Im[f_m] – horizontal plane

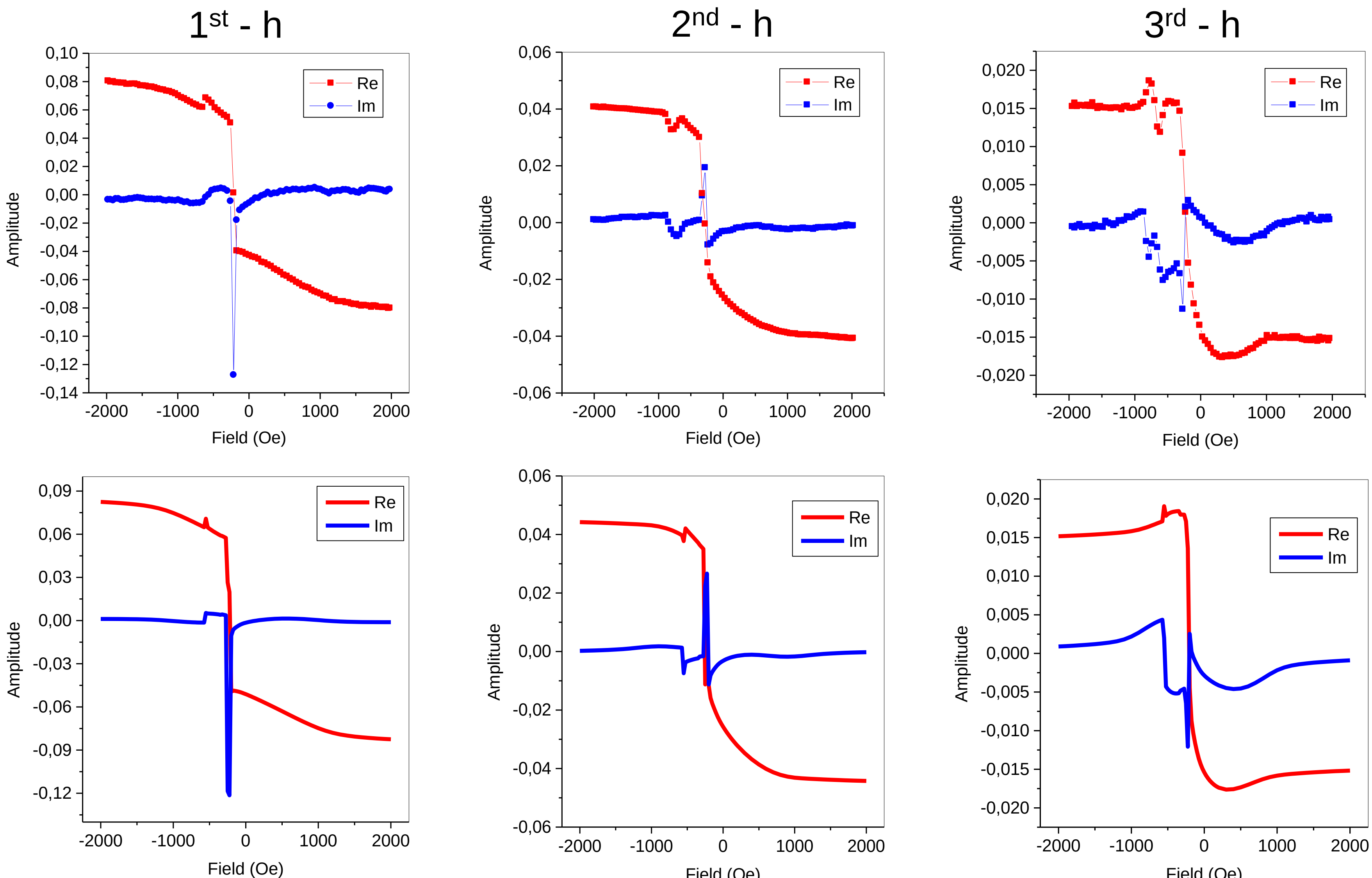

Exp and calculated $Re[f_m]$ and $Im[f_m]$ – vertical plane

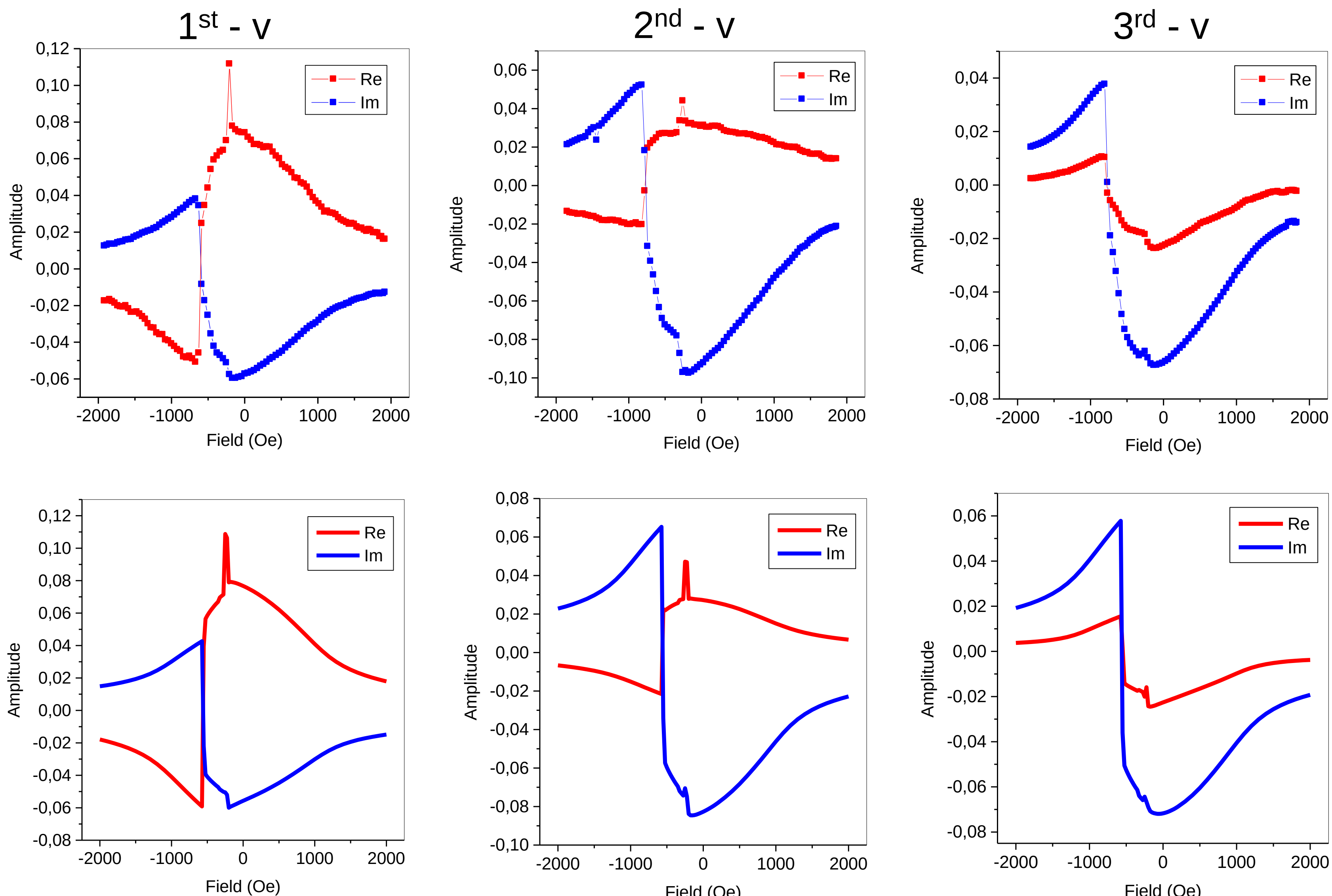

D-MOKE

Micromagnetic simulations

MFM (quenched To 0 field)

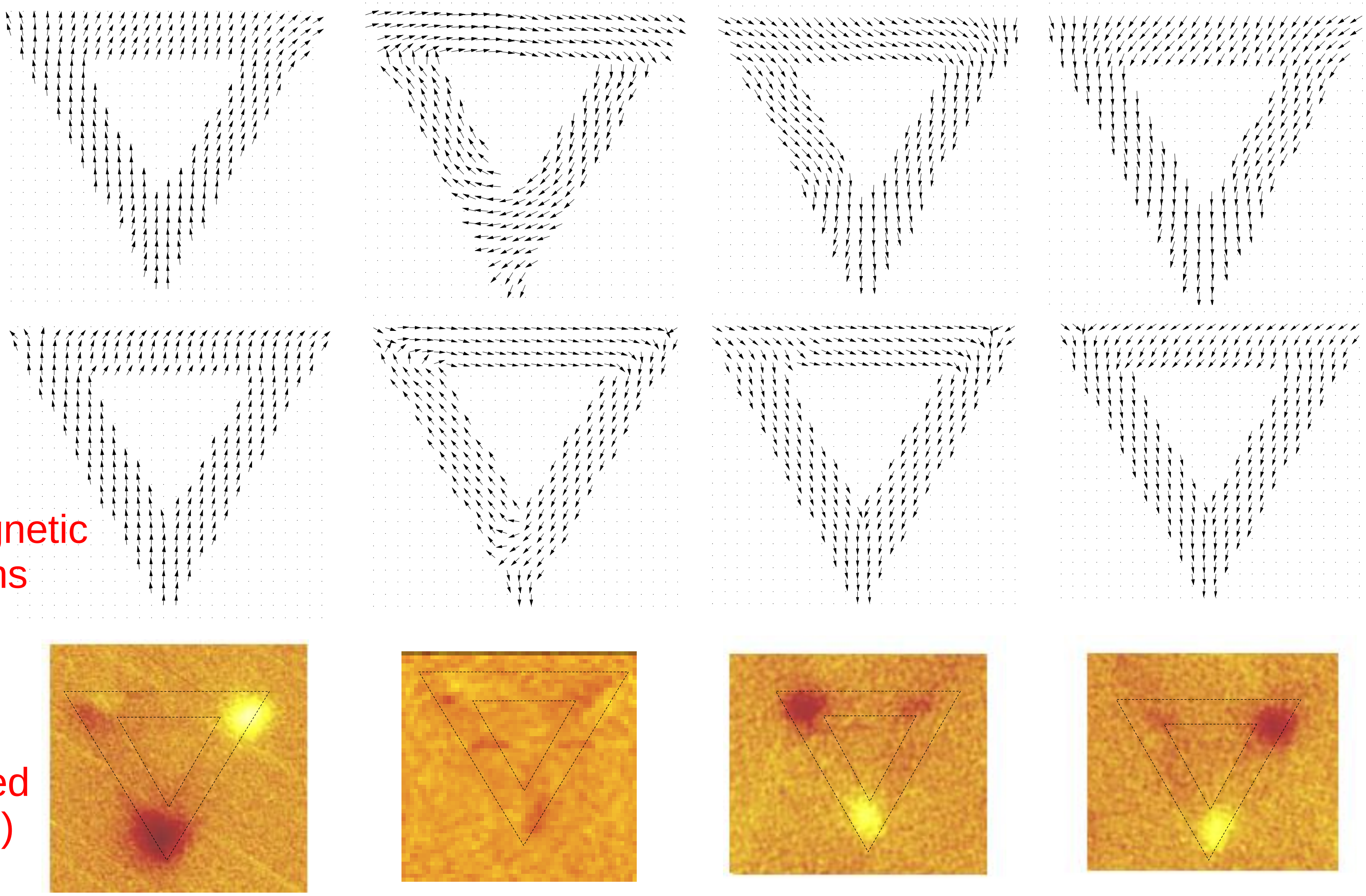

APPLIED PHYSICS LETTERS 99, 092501 (2011)

Concluding remarks

MOKE is a powerful technique for studying technologically relevant magnetic materials.

MOKE magnetometry based on microscopy provides a noninvasive probe of magnetization reversal for individual ultra-small nano-structures.

D-MOKE is a powerful technique to investigate the collective behavior of magnetic nano-arrays.

Next lecture:

Interplay between plasma excitations and MO-activity (magnetoplasmonics).